A Vinyl Silylsilylene and its Activation of Strong Homo- and Heteroatomic Bonds

Matthew M. D. Roy, Michael J. Ferguson, Robert McDonald, Yuqiao Zhou, Eric Rivard*

Contents:

Experimental Procedures:

General

All reactions were performed in an inert atmosphere glovebox (Innovative Technology, Inc.). Solvents (except $Me_3SiOSiMe_3$) were dried using a Grubbs-type solvent purification system[1] manufactured by Innovative Technologies, Inc., degassed (freeze-pump-thaw method), and stored under an atmosphere of nitrogen prior to use. $Me_3SiOSiMe_3$ was degassed (freeze-pump-thaw method) and dried over molecular sieves prior to use. MeOTf was purchased from Aldrich and used as received. $HSiCl_3$, ^tBuNCO, and ^tBuNC were purchased from Aldrich and stored over molecular sieves prior to use. $SiBr_4$ was purchased from Alfa Aesar and used as received. HBpin was purchased from Matrix Scientific and used as received. P_4 was sublimed prior to use. $^{Me}IPr{=}CH_2$ was prepared according to the literature procedure.[2] $[K(THF)_2][Si(SiMe_3)_3]$ was prepared according to the literature procedure and recrystallized from hexanes prior to use.[3] ^1H, $^{11}B\{^1H\}$, $^{13}C\{^1H\}$, $^{29}Si\{^1H\}$, $^{31}P\{^1H\}$ and $^{19}F\{^1H\}$ NMR spectra were recorded on 400, 500, 600 or 700 MHz Varian Inova instruments and were referenced externally to $SiMe_4$ (^1H, $^{13}C\{^1H\}$, $^{29}Si\{^1H\}$), $CFCl_3$ ($^{19}F\{^1H\}$), 85 % H_3PO_4 ($^{31}P\{^1H\}$) or $BF_3{\cdot}Et_2O$ ($^{11}B\{^1H\}$). Elemental analyses were performed by the Analytical and Instrumentation Laboratory at the University of Alberta. Melting points were measured in sealed glass capillaries under nitrogen with a MelTemp apparatus and are uncorrected. UV-visible spectroscopic measurements were carried out with a Varian Carry 300 Scan spectrophotometer. High resolution mass spectra were obtained on an Agilent Technologies 6220 oaTOF (ESI) spectrometer.

X-ray Crystallography

Crystals for X-ray diffraction studies were removed from a vial (in a glovebox) and immediately coated with a thin layer of hydrocarbon oil (Paratone-N). A suitable crystal was then mounted on a glass fiber and quickly placed in a low temperature stream of nitrogen on an X-ray diffractometer.[4] All data were collected using a Bruker APEX II CCD detector/D8 or PLATFORM diffractometer using Mo Kα or Cu Kα radiation, with the crystals cooled to –80 °C or –100 °C. The data were corrected for absorption through

Gaussian integration from the indexing of the crystal faces. Crystal structures were solved using intrinsic phasing (*SHELXT*)[5] and refined using *SHELXL-2014*.[6] The assignment of hydrogen atom positions were based on the sp^2 or sp^3 hybridization geometries of their attached carbon atoms and were given thermal parameters 20 % greater than those of their parent atoms.

Synthesis of (^{Me}IPrCH)SiBr$_3$ (1).

A Schlenk flask charged with a 200 mL diethyl ether solution of ^{Me}IPr=CH$_2$ (3.046 g, 7.073 mmol). SiBr$_4$ (440.7 μL, 3.536 mmol) was added to the stirring solution, immediately affording a flocculent white precipitate. The resulting slurry was stirred overnight and filtered through a glass frit packed with a *ca.* 1 cm plug of Celite. The volatiles of the filtrate were removed *in vacuo*, affording (^{Me}IPrCH)SiBr$_3$ (1.300 g, 53 %) as a microcrystalline, off-white solid. Crystals suitable for X-ray crystallographic analysis were obtained by storing an Et_2O solution of **1** in a −30 °C freezer for one week. ^{1}H NMR (C_6D_6, 699.8 MHz): δ 7.19 (t, 2H, $^3J_{HH}$ = 7.5 Hz, *p*-Ar*H*), 7.10 (d, 4H, $^3J_{HH}$ = 7.5 Hz, *m*-Ar*H*), 3.04 (s, 1H, C*H*SiBr$_3$), 2.94 (broad s, 4H, C*H*(CH$_3$)$_2$), 1.49 (broad s, 12H, CH(C*H*$_3$)$_2$), 1.35 (s, 6H, NCC*H*$_3$), 1.09 (d, 12H, $^3J_{HH}$ = 7.0 Hz, CH(C*H*$_3$)$_2$). ^{13}C{^{1}H} NMR (C_6D_6, 125.7 MHz): δ 152.6 (N*C*N), 148.0 (Ar*C*), 130.8 (Ar*C*), 125.2 (Ar*C*), 119.3 (N*C*-CH$_3$), 54.1 (C=*C*H), 29.0 (*C*H(CH$_3$)$_2$), 24.6 (CH(*C*H$_3$)$_2$), 23.7 (CH(*C*H$_3$)$_2$), 9.4 (NC-*C*H$_3$). *One ArC signal is missing and likely obscured by the C_6D_6 signal.* ^{29}Si{^{1}H} NMR (C_6D_6, 79.5 MHz, DEPT): δ −59.9. Anal. Calcd. for $C_{30}H_{41}Br_3N_2Si$: C 51.66, H 5.93, N 4.02. Found: C 51.46, 5.97, N 3.95. M.p. 202 °C (decomp.)

Synthesis of (^{Me}IPrCH)Si{Si(SiMe$_3$)$_3$} (2).

To a vial containing a 1 mL slurry of (^{Me}IPrCH)SiBr$_3$ (0.168 g, 0.241 mmol) was added a 4 mL solution of [K(THF)$_2$][Si(SiMe$_3$)$_3$] (0.211 g, 0.490 mmol), leading to the immediate formation of a deep green slurry. The resulting mixture was stirred for 20 minutes, filtered and the volatiles were removed from the filtrate *in vacuo*. The resulting deep green solid was washed with 2 x 1.5 mL cold (−30 °C) Me$_3$SiOSiMe$_3$ (to remove the BrSi(SiMe$_3$)$_3$ side-product). The remaining solid was dried *in vacuo*, affording (^{Me}IPrCH)Si{Si(SiMe$_3$)$_3$} as a deep green solid (0.113 g, 67 %). Crystals suitable for X-

ray crystallographic analysis were obtained by storing an $Me_3SiOSiMe_3$ solution of **2** in a −30 °C freezer for two weeks. ^{1}H NMR (C_6D_6, 498.1 MHz): δ 7.40 (s, 1H, satellites: $^2J_{H\text{-}Si}$ = 13.5 Hz, C*H*Si), 7.24 (t, 2H, $^3J_{HH}$ = 8.0 Hz, *p*-Ar*H*), 7.10 (d, 4H, $^3J_{HH}$ = 8.0 Hz, *m*-Ar*H*), 2.88 (sept, 4H, $^3J_{HH}$ = 7.0 Hz, C*H*$(CH_3)_2$), 1.47 (s, 6H, NC-C*H*$_3$), 1.37 (d, 12H, $^3J_{HH}$ = 7.0 Hz), 1.10 (d, 12H, $^3J_{HH}$ = 7.0 Hz), 0.31 (s, 27H, Si$(SiMe_3)_3$). ^{13}C{^{1}H} NMR (C_6D_6, 125.3 MHz): δ 154.4 (N*C*N), 147.0 (Ar*C*), 132.3 (Ar*C*), 130.63 (Ar*C*), 128.3 (C=*C*H), 125.3 (Ar*C*), 121.0 (N*C*-CH_3), 29.2 (*C*H$(CH_3)_2$), 24.6 (CH(*C*$H_3)_2$, 23.8 (CH(*C*H_3), 9.1 (NC-*C*H_3), 3.85 (Si$(SiMe_3)_3$). ^{29}Si{^{1}H} NMR (C_6D_6, 79.5 MHz, DEPT): δ 432.9 (*Si*-Si$(SiMe_3)_3$), −9.5 (Si-Si(*Si*$Me_3)_3$), −113.4 (Si-*Si*$(SiMe_3)_3$). Anal. Calcd. for $C_{39}H_{68}N_2Si_5$: C 66.41, H 9.72, N 3.97. Found: C 65.58, H 9.69, N 3.89. M.p. 110–112 °C. UV-Vis: λ_{max} = 266 nm (ε = 8630 $M^{-1}cm^{-1}$), 309 nm (ε = 9500 $M^{-1}cm^{-1}$), 416 nm (ε = 3130 $M^{-1}cm^{-1}$), 583 (ε = 42 $M^{-1}cm^{-1}$).

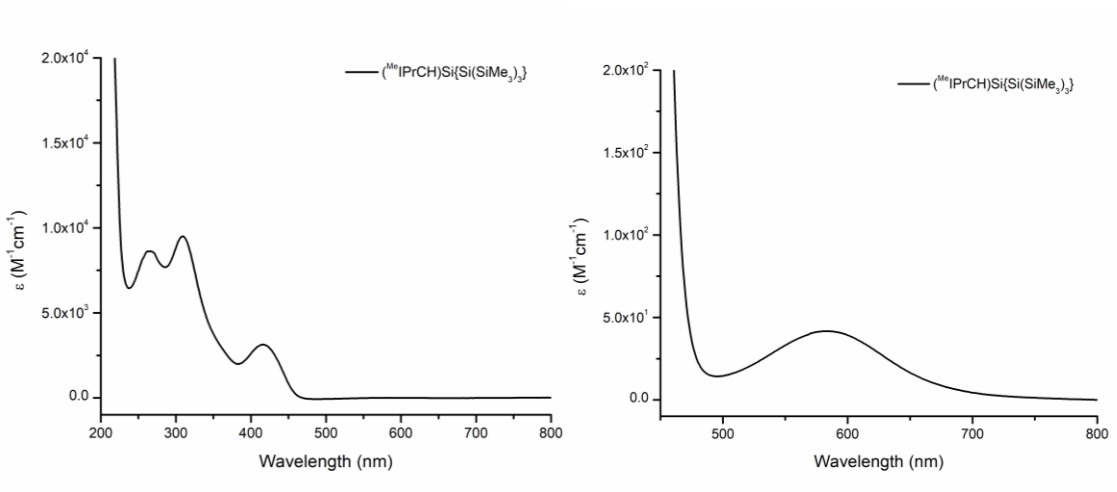

Figure S1. UV-Visible spectrum of (^{Me}IPrCH)Si{Si$(SiMe_3)_3$} (**2**) in hexanes of a 3.54×10^{-5} M solution (left) and a 3.40×10^{-3} M solution (right).

Synthesis of (^{Me}IPrCH)Si(Me)OTf{Si(SiMe$_3$)$_3$} (3).

To a vial containing a 1.5 mL benzene solution of **2** (0.042 g, 0.060 mmol) was added MeOTf (6.60 μL, 0.060 mmol). The resulting colorless solution was stirred for 30 seconds and the volatiles were removed *in vacuo* affording (^{Me}IPrCH)Si(Me)OTf{Si(SiMe$_3$)$_3$} as a colorless solid (0.048 g, 93 %). Crystals suitable for X-ray crystallographic analysis were grown by the slow evaporation of a 1:1 benzene:hexanes solution of **3** at room temperature. ^{1}H NMR (C$_6$D$_6$, 399.8 MHz): δ 7.30-7.20 (m, 4H, *m*-ArH), 7.13-7.03 (m, 2H, *p*-ArH), 3.53 (sept, 2H, $^3J_{HH}$ = 6.4 Hz, C*H*(CH$_3$)$_2$), 3.00 (sept, 1H, $^3J_{HH}$ = 6.4 Hz, C*H*(CH$_3$)$_2$), 2.75 (sept, 1H, $^3J_{HH}$ = 6.4 Hz, C*H*(CH$_3$)$_2$), 2.72 (s, 1H, C*H*Si), 1.66 (d, 3H, $^3J_{HH}$ = 6.4 Hz, CH(C*H*$_3$)$_2$), 1.55 (d, 3H, $^3J_{HH}$ = 6.4 Hz, CH(C*H*$_3$)$_2$), 1.37 (s, 3H, NC-C*H*$_3$), 1.33 (s, 3H, NC-C*H*$_3$), 1.31 (d, 6H, $^3J_{HH}$ = 6.4 Hz, CH(C*H*$_3$)$_2$), 1.15 (d, 3H, $^3J_{HH}$ = 6.4 Hz, CH(C*H*$_3$)$_2$), 1.12 (d, 3H, $^3J_{HH}$ = 6.4 Hz, CH(C*H*$_3$)$_2$), 1.10 (d, 3H, $^3J_{HH}$ = 6.4 Hz, CH(C*H*$_3$)$_2$), 1.09 (d, 3H, $^3J_{HH}$ = 6.4 Hz, CH(C*H*$_3$)$_2$), 0.99 (d, 3H, $^3J_{HH}$ = 6.4 Hz, CH(C*H*$_3$)$_2$), 0.24 (s, 27H, Si(SiMe$_3$)$_3$), −0.28 (s, 3H, Si-C*H*$_3$). ^{13}C{^{1}H} NMR (C$_6$D$_6$, 176.0 MHz): δ 154.1 (N*C*N), 149.5 (Ar*C*), 148.7 (Ar*C*), 147.7 (Ar*C*), 147.4 (Ar*C*), 134.7 (Ar*C*), 132.6 (Ar*C*), 130.3 (Ar*C*), 129.9 (Ar*C*), 128.5 (Ar*C*), 128.3 (Ar*C*), 125.6 (Ar*C*), 125.4 (Ar*C*), 124.8 (Ar*C*), 120.1 (N*C*-CH$_3$), 119.6 (N*C*-CH$_3$), 48.7 (C=*C*H), 28.6 (*C*H(CH$_3$)$_2$), 28.5 (*C*H(CH$_3$)$_2$), 28.2 (*C*H(CH$_3$)$_2$, 26.2 (*C*H$_3$), 25.1 (*C*H$_3$), 24.1 (*C*H$_3$), 23.6 (*C*H$_3$), 23.4 (*C*H$_3$), 23.3 (*C*H$_3$), 10.3 (*C*H$_3$), 10.2 (*C*H$_3$), 4.9 (Si-*C*H$_3$), 3.3 (Si(SiMe$_3$)$_3$). ^{29}Si{^{1}H} NMR (C$_6$D$_6$, 79.5 MHz, DEPT): δ 26.8 (*Si*-Si(SiMe$_3$)$_3$), −10.5 (Si-Si(*Si*Me$_3$)$_3$), −125.0 (Si-*Si*(SiMe$_3$)$_3$). ^{19}F{^{1}H} NMR (C$_6$D$_6$, 376.3 MHz): δ −75.8. Anal. Calcd. for C$_{41}$H$_{71}$F$_3$N$_2$O$_3$SSi$_5$: C 56.64, H 8.23, N 3.22 S 3.69. Found: C 55.52, H 8.11, N 3.06, S 3.10. M.p. 240 °C (decomp.; turns red).

Synthesis of (^{Me}IPrCH)Si(H)Bpin{Si(SiMe$_3$)$_3$} (4).

To a vial containing a 1 mL solution of **2** (0.024 g, 0.034 mmol) in toluene was added HBpin (4.9 μL, 0.034 mmol). The deep green color of **2** began to lighten upon the addition of HBpin, eventually turning to a pale-yellow color after 5 minutes of stirring. The resulting solution was stirred for an additional 30 minutes and the volatiles were subsequently removed *in vacuo* yielding a pale-yellow oil. The oil was triturated with 0.5 mL hexanes and dried *in vacuo*, affording (^{Me}IPrCH)Si(H)Bpin{Si(SiMe$_3$)$_3$} as a pale-

yellow solid (0.017 g, 60 %). ^{1}H NMR (C_6D_6, 498.1 MHz): δ 7.30-7.18 (m, 6H, *m*-Ar*H*/*p*-Ar*H*), 3.61 (d, 1H, $^{3}J_{HH}$ = 9.3 Hz, satellites: $^{1}J_{H\text{-}Si}$ = 180.0 Hz, Si-*H*), 3.50 (sept, 1H, $^{3}J_{HH}$ = 6.5 Hz, C*H*(CH_3)$_2$), 3.37 (sept, 1H, $^{3}J_{HH}$ = 6.5 Hz, C*H*(CH_3)$_2$), 3.12-3.04 (m, 2H, C*H*(CH_3)$_2$), 1.72 (d, 1H, $^{3}J_{HH}$ = 9.3 Hz, C=C*H*), 1.57-1.49 (m, 12H, CH(C*H*$_3$)$_2$ and NCC*H*$_3$), 1.39 (d, 3H, $^{3}J_{HH}$ = 7.0 Hz, CH(C*H*$_3$)$_2$), 1.25 (d, 3H, $^{3}J_{HH}$ = 6.5 Hz, CH(C*H*$_3$)$_2$), 1.20-1.15 (m, 12H, CH(C*H*$_3$)$_2$), 1.10 (s, 6H, Bpin), 1.08 (s, 6H, Bpin), 0.30 (s, 27H, Si(SiMe$_3$)$_3$). ^{13}C{^{1}H} NMR (C_6D_6, 176.0 MHz): δ 153.7 (N*C*N), 149.3 (Ar*C*), 148.2 (Ar*C*), 134.6 (Ar*C*), 133.7 (Ar*C*), 129.5 (Ar*C*), 129.2 (Ar*C*), 124.7 (Ar*C*), 124.6 (Ar*C*), 124.5 (Ar*C*), 123.9 (Ar*C*), 117.7 (N*C*CH$_3$), 117.6 (N*C*CH$_3$), 82.7 (BO*C*, Bpin), 34.7 (C=*C*H), 29.0 (*C*(CH_3)$_2$), 28.8 (*C*(CH_3)$_2$, 28.7 (*C*(CH_3)$_2$, 28.4 (*C*(CH_3)$_2$, 26.9 (*C*H$_3$), 26.3 (*C*H$_3$), 25.2 (*C*H$_3$), 24.8 (*C*H$_3$), 24.8 (*C*H$_3$), 24.2 (*C*H$_3$), 23.8 (*C*H$_3$), 23.6 (*C*H$_3$), 23.2 (*C*H$_3$), 10.3 (*C*H$_3$, Bpin), 10.0 (*C*H$_3$, Bpin), 3.5 (Si(SiMe$_3$)$_3$. ^{11}B{^{1}H} 33.8 (broad s, *B*pin). ^{29}Si{^{1}H} NMR (C_6D_6, 79.5 MHz, DEPT): δ −0.5 (*Si*-Si(SiMe$_3$)$_3$), −9.6 (Si-Si(*Si*Me$_3$)$_3$), −119.0 (Si-*Si*(SiMe$_3$)$_3$). Anal. Calcd. for $C_{45}H_{81}BN_2O_2Si_5$: C 64.85, H 9.80, N 3.36. Found: C 64.49, H 9.68, N 3.35. M.p. 194 °C (decomp.) HRMS (ESI in THF): m/z calculated for $C_{45}H_{81}{}^{11}BN_2O_2Si_5$: 833.5310; Found: 833.5313 (Δppm = 0.37).

Synthesis of (^{Me}IPrCH)ClSi(HSiCl$_2$){Si(SiMe$_3$)$_3$} (5).

To a vial containing a 1 mL toluene solution of **2** (0.021 g, 0.030 mmol) was added $HSiCl_3$ (3.0 μL, 0.030 mmol). The resultant pale-yellow solution was stirred for 20 minutes and the volatiles were removed *in vacuo* affording a pale-yellow solid. The solid was re-dissolved in C_6D_6 for NMR analysis, revealing the quantitative formation of **5**. The NMR solution was then transferred to a vial and dried *in vacuo* affording (^{Me}IPrCH)ClSi(HSiCl$_2$){Si(SiMe$_3$)$_3$} as a pale-yellow solid (0.019 g, 76 %). Crystals suitable for X-ray crystallographic analysis were obtained by slow evaporation of a hexanes solution of **5** over one week at room temperature. ^{1}H NMR (C_6D_6, 399.8 MHz): δ 7.24-7.08 (m, 6H, *m*-Ar*H*/*p*-Ar*H*), 4.64 (s, 1H, satellites: $^{1}J_{H\text{-}Si}$ = 248.4 Hz, $^{2}J_{H\text{-}Si}$ = 23.4 Hz, Si-*H*), 3.30 (broad s, 1H, C*H*(CH_3)$_2$), 3.14 (broad s, 2H, C*H*(CH_3)$_2$), 2.85 (broad sept, 1H, $^{3}J_{HH}$ = 5.6 Hz, C*H*(CH_3)$_2$), 2.53 (s, 1H, satellites: $^{2}J_{H\text{-}Si}$ = 55.6 Hz, $^{3}J_{H\text{-}Si}$ = 7.0 Hz, C*H*Si), 1.51 (broad s, 6H, CH(C*H*$_3$)$_2$), 1.43 (broad s, 6H, CH(C*H*$_3$)$_2$), 1.31 (broad s, 3H, NC-C*H*$_3$), 1.27 (broad s, 3H, NC-C*H*$_3$), 1.10 (broad d, 6H, $^{3}J_{HH}$ = 5.6 Hz, CH(C*H*$_3$)$_2$),

1.04 (broad s, 6H, CH(C*H*$_3$)$_2$), 0.32 (s, 27H, Si(SiMe$_3$)$_3$). ^{29}Si{^{1}H} NMR (C_6D_6, 79.5 MHz, DEPT): δ −0.5 (H*Si*Cl$_2$), −9.6 (Si-Si(*Si*Me$_3$)$_3$), −13.4 (*Si*-Si(SiMe$_3$)$_3$), −118.9 (Si-*Si*(SiMe$_3$)$_3$). *Due to significant broadening caused by hindered rotation of the -Dipp groups, a ^{13}C{^{1}H} spectrum was not recorded at room temperature. As such, ^{1}H and ^{13}C{^{1}H} spectra were recorded at +75 °C to resolve this broadening:* ^{1}H NMR (C_6D_6, 399.8 MHz, +75 °C): δ 7.24-7.17 (m, 6H, *m*-Ar*H*/*p*-Ar*H*), 4.81 (s, 1H, satellites: $^1J_{H\text{-}Si}$ = 248.4 Hz, $^2J_{H\text{-}Si}$ = 23.4 Hz, Si-*H*), 3.20 (sept, 2H, $^3J_{HH}$ = 6.8 Hz, C*H*(CH$_3$)$_2$), 3.04 (sept, 2H, $^3J_{HH}$ = 6.8 Hz, C*H*(CH$_3$)$_2$), 2.48 (s, 1H, satellites: $^2J_{H\text{-}Si}$ = 55.6 Hz, $^3J_{H\text{-}Si}$ = 7.0 Hz, C*H*Si), 1.46 (d, 12H, $^3J_{HH}$ = 6.8 Hz), 1.36 (s, 6H, NC-C*H*$_3$), 1.12 (d, 6H $^3J_{HH}$ = 6.8 Hz), 1.06 (d, 6H, $^3J_{HH}$ = 6.8 Hz), 0.29 (s, 27H, Si(SiMe$_3$)$_3$). ^{13}C{^{1}H} NMR (C_6D_6, 100.6 MHz, +75 °C): δ 155.5 (N*C*N), 148.2 (Ar*C*), 130.3 (Ar*C*), 125.6 (Ar*C*), 125.5 (Ar*C*), 120.5 (N*C*CH$_3$), 43.2 (C=*C*H), 29.0 (*C*H(CH$_3$)$_2$), 28.8 (*C*H(CH$_3$)$_2$), 25.8 (CH(*C*H$_3$)$_2$), 24.9 (CH(*C*H$_3$)$_2$), 23.8 (CH(*C*H$_3$)$_2$), 23.7 (CH(*C*H$_3$)$_2$), 10.3 (NC-*C*H$_3$), 4.1 (Si(SiMe$_3$)$_3$). Anal. Calcd. for $C_{39}H_{69}Cl_3N_2Si_6$: C 55.71, H 8.27, N 3.33. Found: C 55.72, H 8.26, N 3.29. M.p. 218 °C (decomp.; turns red).

Synthesis of (^{Me}IPrCH)Si(P$_4$){Si(SiMe$_3$)$_3$} (6).

Route A:

To a vial containing a 1 mL slurry of (^{Me}IPrCH)SiBr$_3$ (0.088 g, 0.126 mmol) in toluene was added a 3 mL toluene solution of [K(THF)$_2$][Si(SiMe$_3$)$_3$] (0.108 g, 0.251 mmol), immediately forming a deep green slurry (containing silylene **2** and BrSi(SiMe$_3$)$_3$). After stirring the mixture for 5 min. a 2 mL solution of P$_4$ (0.016 g, 0.129 mmol) in toluene was added. After two minutes of stirring, the mixture had changed from deep green to a red color. The mixture was stirred for an additional 20 min. after which the color had lightened to orange. The slurry was filtered and the volatiles were removed from the filtrate *in vacuo*. The solid residue was washed with 2 mL Me$_3$SiOSiMe$_3$ and dried *in vacuo*, affording (^{Me}IPrCH)Si(P$_4$){Si(SiMe$_3$)$_3$} as a pale yellow/orange solid (0.046 g, 44 %). Crystals suitable for X-ray crystallographic analysis were grown by storing a hexanes solution of **6** in a −30 °C freezer overnight. ^{1}H NMR (C_6D_6, 400.0 MHz): δ 7.49-7.34 (m, 4H, *m*-Ar*H*), 7.15-7.07 (m, 2H, *o*-Ar*H*), 3.47 (broad sept, 2H, $^3J_{HH}$ = 5.6 Hz, C*H*(CH$_3$)$_2$), 3.31 (s, 1H, C*H*Si), 3.05 (broad sept, 2H, $^3J_{HH}$ = 5.6 Hz, C*H*(CH$_3$)$_2$), 1.78 (broad d, 6H,

$^{3}J_{HH}$ = 5.6 Hz, CH(CH_3)$_2$), 1.39 (s, 6H, NC-CH_3), 1.36 (broad d, 6H, $^{3}J_{HH}$ = 5.6 Hz, CH(CH_3)$_2$), 1.21 (broad d, 6H, $^{3}J_{HH}$ = 5.6 Hz, CH(CH_3)$_2$), 1.10 (broad d, 6H, $^{3}J_{HH}$ = 5.6 Hz, CH(CH_3)$_2$), 0.42 (s, 27H, Si(SiMe$_3$)$_3$). ^{29}Si{^{1}H} NMR (C_6D_6, 79.4 MHz, DEPT): δ −9.4 (s, Si-Si(*Si*Me$_3$)$_3$), −10.0 (m, *Si*-Si(SiMe$_3$)$_3$), −109.6 (broad s, Si-*Si*(SiMe$_3$)$_3$). ^{31}P{^{1}H} NMR (C_6D_6, 161.9 MHz): δ 120.0 (dd, $^{1}J_{P1-P2}$ = 158.2 Hz, $^{2}J_{P1-P3}$ = 150.6 Hz, P1), −181.0 (dt, $^{1}J_{P3-P2}$ = 165.1 Hz, $^{2}J_{P3-P1}$ = 150.6 Hz, P3), −316.7 (dt, $^{1}J_{P2-P3}$ = 165.1, $^{1}J_{P2-P1}$ = 158.2 Hz, P2). (See Figure S26 for an assigned ^{31}P{^{1}H} NMR spectrum). *Due to significant broadening, we were unable to collect suitable ^{13}C{^{1}H} NMR data at room temperature, +75 °C (C_6D_6) or +100 °C (toluene-d_8).* Anal. Calcd. for $C_{39}H_{68}N_2P_4Si_5$: C 56.48, H 8.27, N 3.38. Found: C 55.97, H 8.18, N 3.26. M.p. 184–186°C (melts to red).

Route B:

To a vial containing a 1 mL solution of **2** (0.066 g, 0.094 mmol) in toluene was added a 2 mL toluene solution of P_4 (0.012 g, 97 mmol). After two minutes of stirring, the solution had changed from deep green to a red color. The solution was stirred for an additional 30 min. after which the color had lightened to orange. The volatiles were removed *in vacuo*, affording (^{Me}IPrCH)Si(P_4){Si(SiMe$_3$)$_3$} as a pale yellow/orange solid (0.064 g, 82 %).

Synthesis of (^{Me}IPrCH)SiH(CN){Si(SiMe$_3$)$_3$} (7) from ^{t}BuNCO.

To a vial containing a 1 mL toluene solution of **2** (0.050 g, 0.071 mmol) was added ^{t}BuNCO (4.20 μL, 0.037 mmol) with no discernable color change upon addition. The mixture was stirred overnight, resulting in a pale-yellow solution. The volatiles were removed *in vacuo*, the residue extracted with 1 mL hexanes and the solution placed in a −30 °C freezer overnight affording pale-yellow crystals, from which a few crystals were removed for X-ray crystallographic analysis. The mother liquor was decanted from the bulk sample and the volatiles were removed *in vacuo*, yielding (^{Me}IPrCH)SiH(CN){Si(SiMe$_3$)$_3$} as a pale-yellow crystalline solid (0.008 g, 31 %). ^{1}H NMR (C_6D_6, 699.7 MHz): δ 7.36-7.32 (m, 2H, Ar*H*), 7.27-7.24 (m, 1H, Ar*H*), 7.20-7.13 (m, 3H, Ar*H*), 3.92 (d, 1H, $^{3}J_{HH}$ = 7.7 Hz, satellites: $^{1}J_{H-Si}$ = 210.7 Hz, Si-*H*), 3.22 (sept, 1H, $^{3}J_{HH}$ = 7.0 Hz, C*H*(CH$_3$)$_2$), 3.10 (sept, 2H, $^{3}J_{HH}$ = 7.0 Hz, C*H*(CH$_3$)$_2$), 2.91 (sept, 1H, $^{3}J_{HH}$ = 7.0 Hz, C*H*(CH$_3$)$_2$), 1.78 (d, 3H, $^{3}J_{HH}$ = 7.0 Hz, C*H*(CH$_3$)$_2$), 1.75 (d, 1H, $^{3}J_{HH}$ = 7.7 Hz, C*H*(CH$_3$)$_2$), 1.54 (d, 3H, $^{3}J_{HH}$ = 7.0 Hz, CH(CH_3)$_2$), 1.47 (s, 3H, NC-CH_3), 1.46 (s,

3H, NC-CH_3), 1.43 (d, 3H, $^3J_{HH}$ = 7.0 Hz, CH(CH_3)$_2$), 1.32 (d, 3H, $^3J_{HH}$ = 7.0 Hz, CH(CH_3)$_2$), 1.18 (d, 3H, $^3J_{HH}$ = 7.0 Hz, CH(CH_3)$_2$), 1.13 (d, 3H, $^3J_{HH}$ = 7.0 Hz, CH(CH_3)$_2$), 1.11 (d, 3H, $^3J_{HH}$ = 7.0 Hz, CH(CH_3)$_2$), 1.10 (d, 3H, $^3J_{HH}$ = 7.0 Hz, CH(CH_3)$_2$), 0.25 (s, 27H, Si(SiMe$_3$)$_3$). ^{13}C{^{1}H} NMR (C_6D_6, 176.0 MHz): δ 154.7 (N*C*N), 148.9 (Ar*C*), 148.7 (Ar*C*), 148.3 (Ar*C*), 147.8 (Ar*C*), 133.0 (Ar*C*), 132.5 (Ar*C*), 130.7 (Ar*C*), 129.8 (Ar*C*), 128.3 (Si-*C*N), 126.2 (Ar*C*), 124.9 (Ar*C*), 124.6 (Ar*C*), 124.1 (Ar*C*), 118.6 (N*C*-CH$_3$), 118.2 (N*C*-CH$_3$), 32.4 (C=*C*H), 29.4 (*C*H(CH$_3$)$_2$), 28.8 (*C*H(CH$_3$)$_2$), 28.7 (*C*H(CH$_3$)$_2$), 25.6 (*C*H$_3$), 25.1 (*C*H$_3$), 24.3 (*C*H$_3$) 24.2 (*C*H$_3$), 24.1 (*C*H$_3$), 23.9 (*C*H$_3$), 23.8 (*C*H$_3$), 23.2 (*C*H$_3$), 2.7 (Si(SiMe$_3$)$_3$). ^{29}Si{^{1}H} NMR (C_6D_6, 79.4 MHz, DEPT): δ −9.7 (s, Si-Si(*Si*Me$_3$)$_3$), −74.5 (*Si*-Si(SiMe$_3$)$_3$), −133.0 (Si-*Si*(SiMe$_3$)$_3$). Anal. Calcd. for $C_{40}H_{69}N_3Si_5$: C 65.59, H 9.50, N 5.74. Found C 64.99, H 9.16, N 6.16. M.p. 158 °C (decomp.) HRMS (ESI in THF): m/z calculated for $C_{40}H_{69}N_3Si_5$: 732.4411; Found: 732.4400 (Δppm = 1.5).

Synthesis of (^{Me}IPrCH)SiH(CN){Si(SiMe$_3$)$_3$} (7) from ^{t}BuNC.

A J. Young PTFE valve-capped NMR tube was loaded with a 0.5 mL solution of **2** (0.014 g, 0.020 mmol) to which ^{t}BuNC was added (2.24 μL, 0.0198 mmol). Upon addition, the deep green color of **2** immediately dissipated, forming a pale-yellow solution. After NMR analysis (which revealed a mixture of **7** and isobutylene), the solution was transferred to a vial and the volatiles were removed *in vacuo*, affording (^{Me}IPrCH)SiH(CN){Si(SiMe$_3$)$_3$} (**7**) as a pale-yellow solid (0.013 g, 89 %).

NMR Spectra

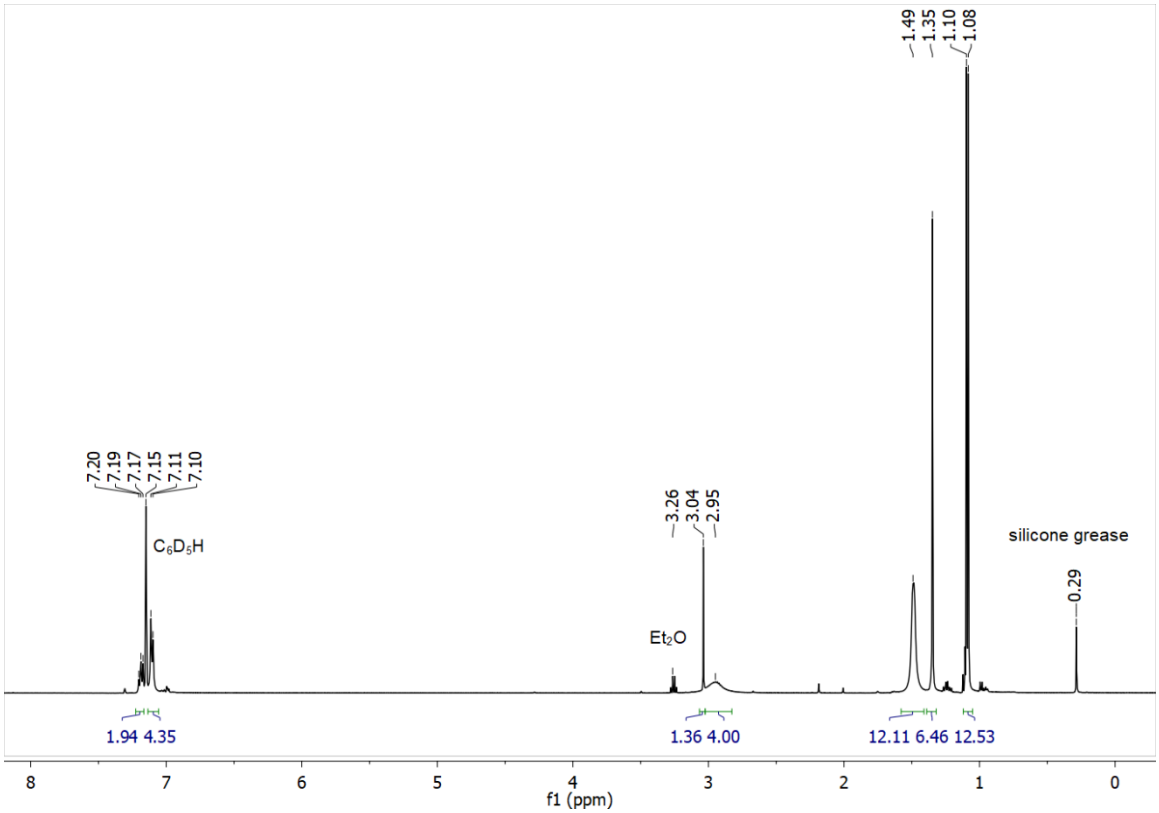

Figure S2. ^{1}H NMR spectrum of (^{Me}IPrCH)SiBr$_3$ (**1**) in C_6D_6.

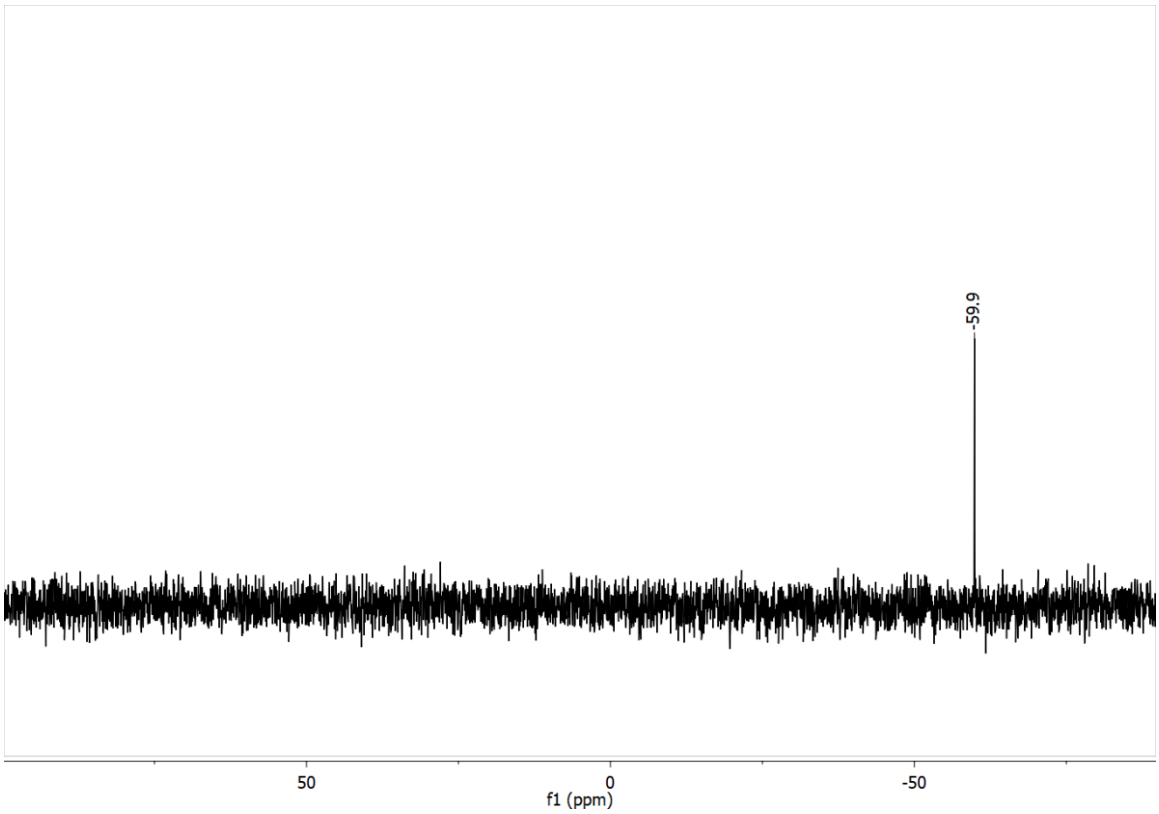

Figure S3. $^{29}Si\{^{1}H\}$ DEPT NMR spectrum of (^{Me}IPrCH)$SiBr_3$ (**1**) in C_6D_6 optimized for 7 Hz scalar coupling (1 adjacent proton).

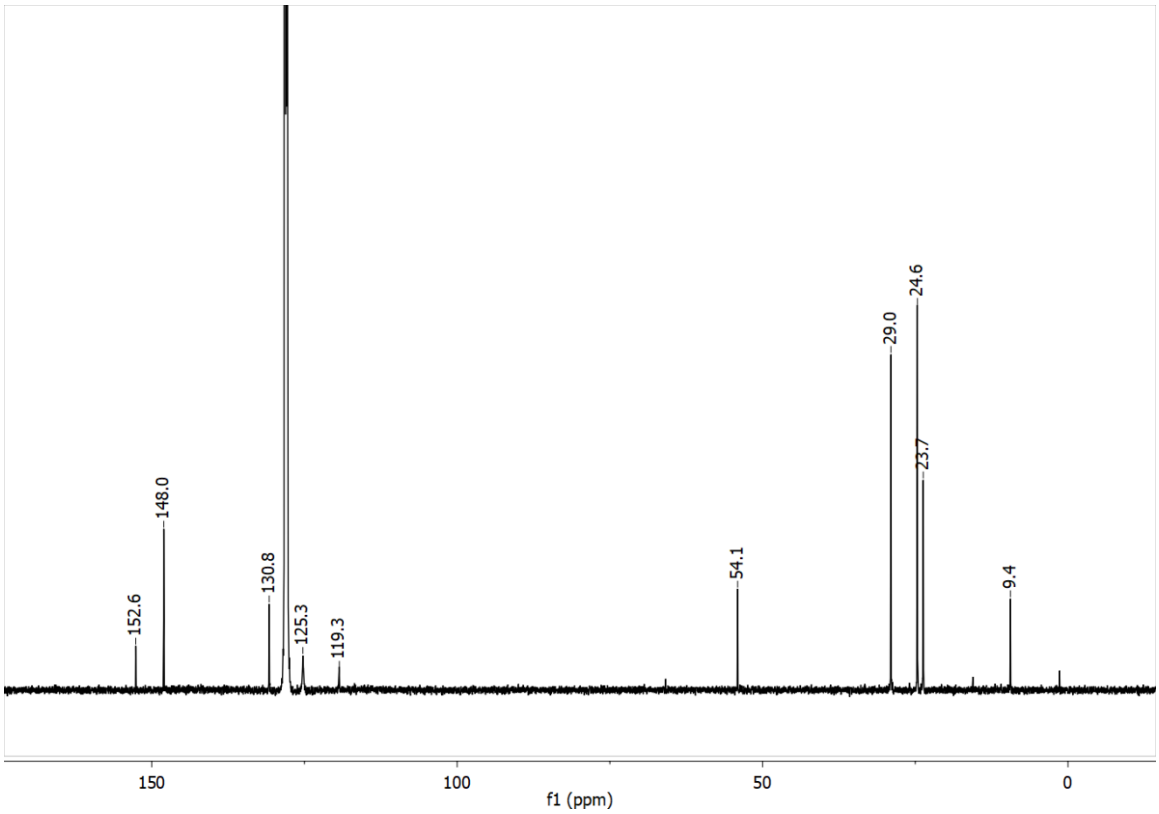

Figure S4. $^{13}C\{^{1}H\}$ NMR spectrum of (^{Me}IPrCH)SiBr$_3$ (**1**) in C_6D_6.

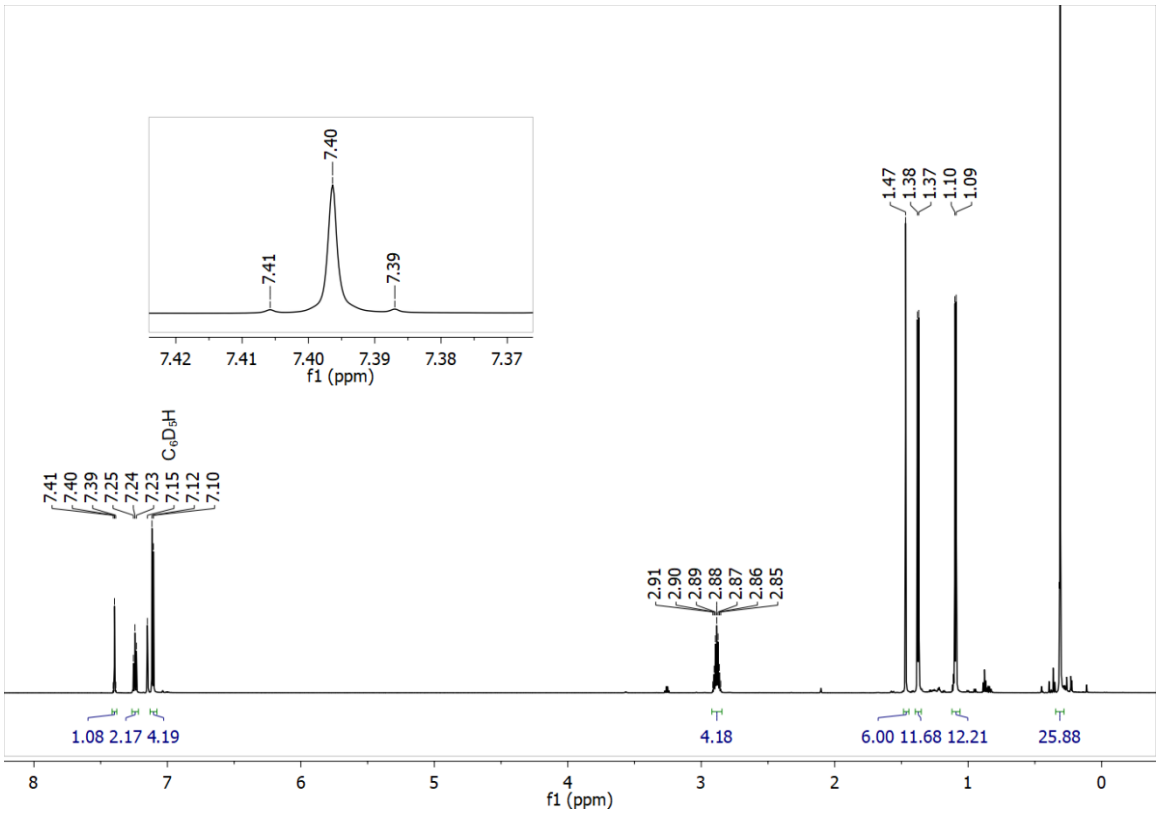

Figure S5. ^{1}H NMR spectrum of (^{Me}IPrCH)Si{Si(SiMe$_3$)$_3$} (**2**) in C_6D_6.

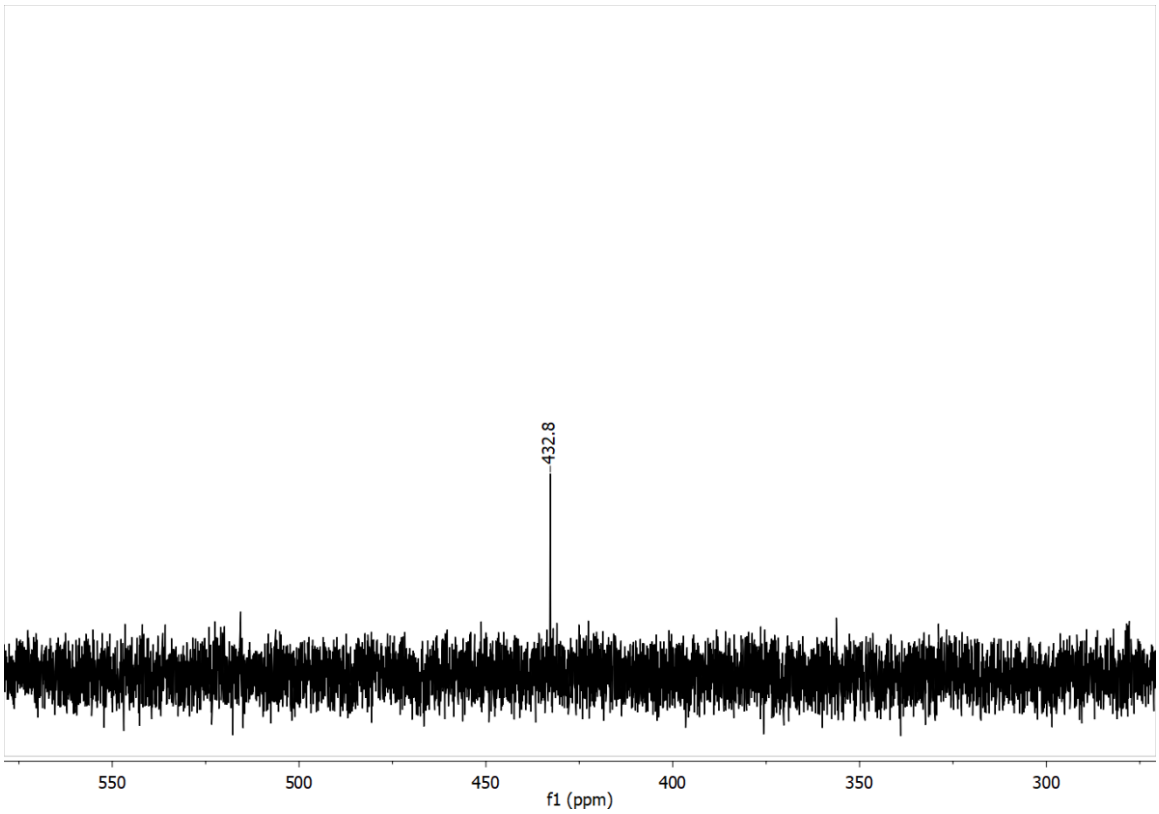

Figure S6. $^{29}Si\{^{1}H\}$DEPT NMR spectrum of (^{Me}IPrCH)Si{Si(SiMe$_3$)$_3$} (**2**) in C_6D_6 optimized for 13 Hz scalar coupling (1 adjacent proton).

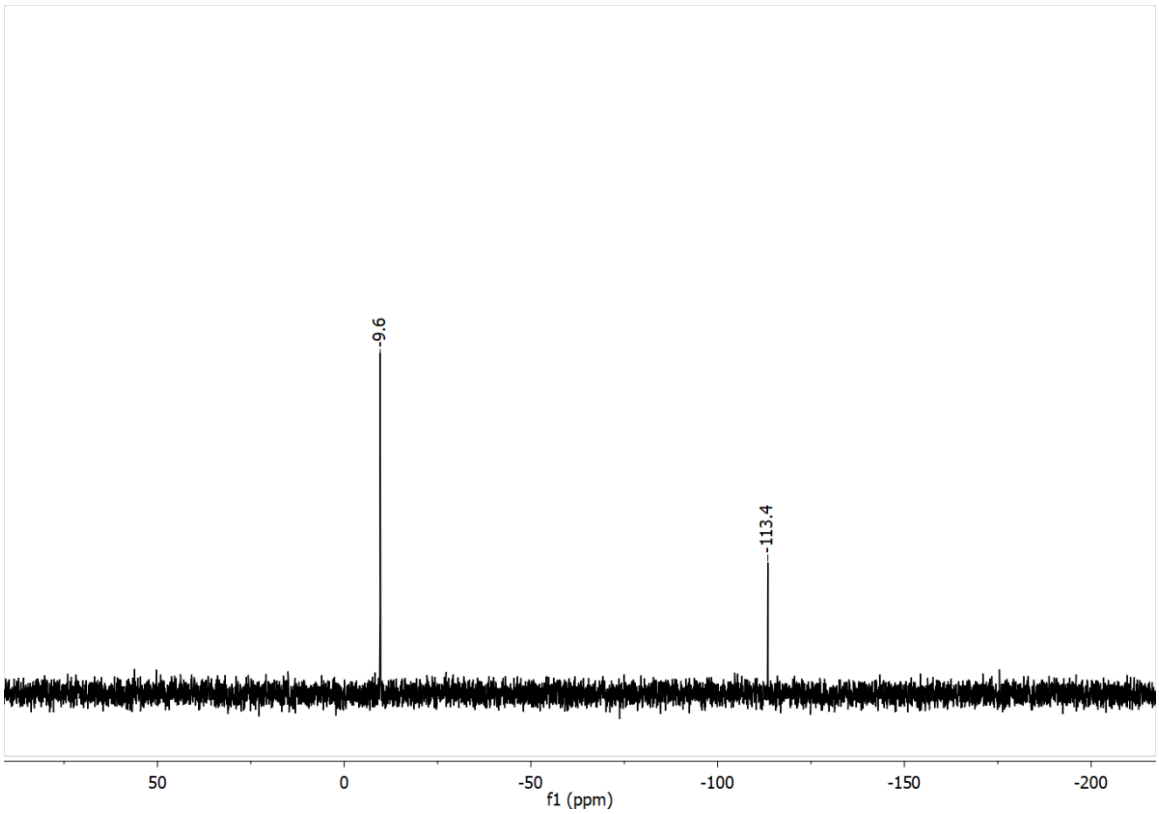

Figure S7. $^{29}Si\{^{1}H\}$ DEPT NMR spectrum of (^{Me}IPrCH)Si{Si(SiMe$_3$)$_3$} (**2**) in C_6D_6 optimized for 7 Hz scalar coupling (9 adjacent protons).

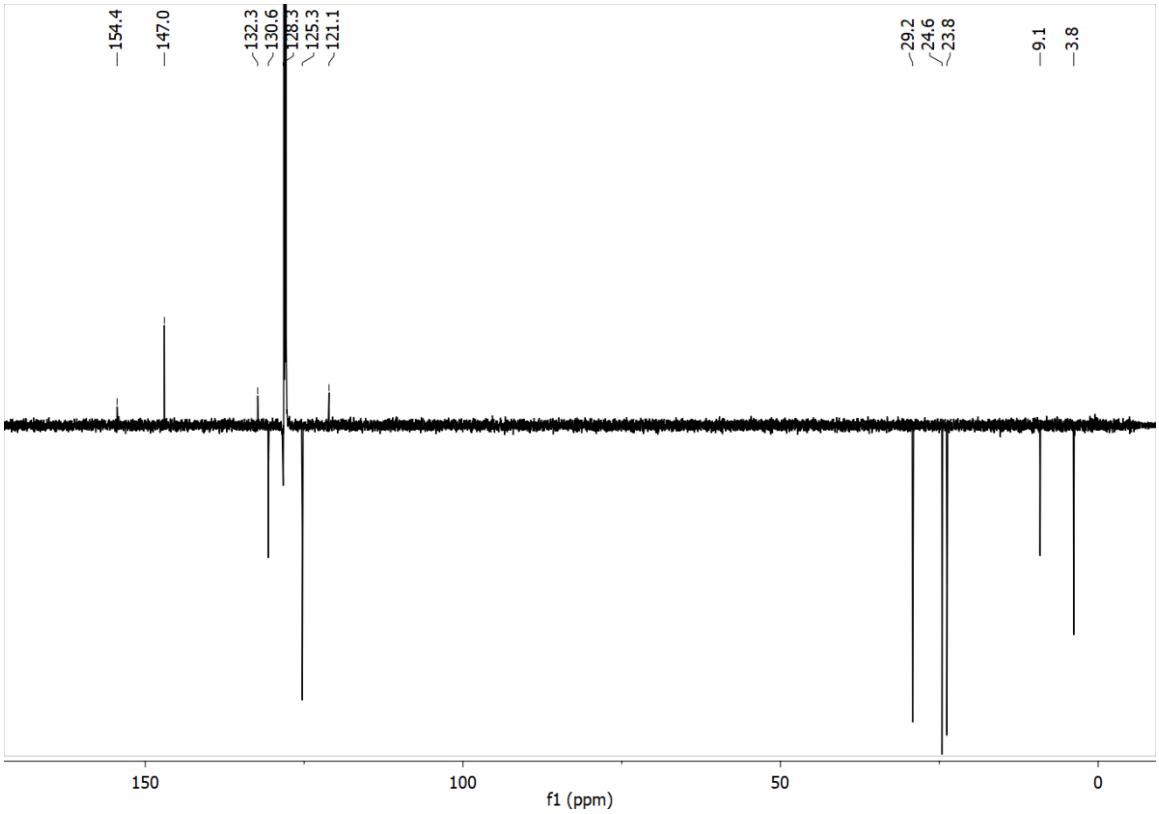

Figure S8. $^{13}C\{^{1}H\}$ DEPT NMR spectrum of (^{Me}IPrCH)Si{Si(SiMe$_3$)$_3$} (**2**) in C_6D_6.

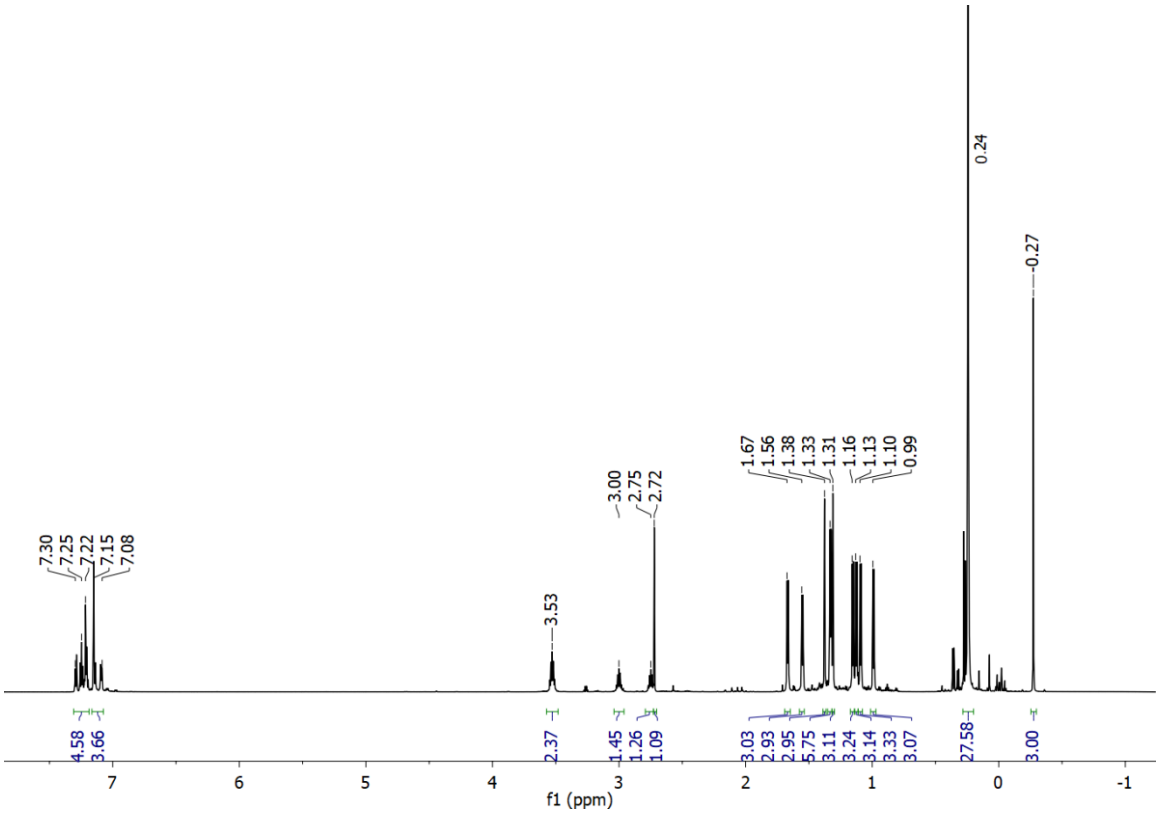

Figure S9. ^{1}H NMR spectrum of (^{Me}IPrCH)Si(Me)OTf{Si(SiMe$_3$)$_3$} (**3**) in C_6D_6.

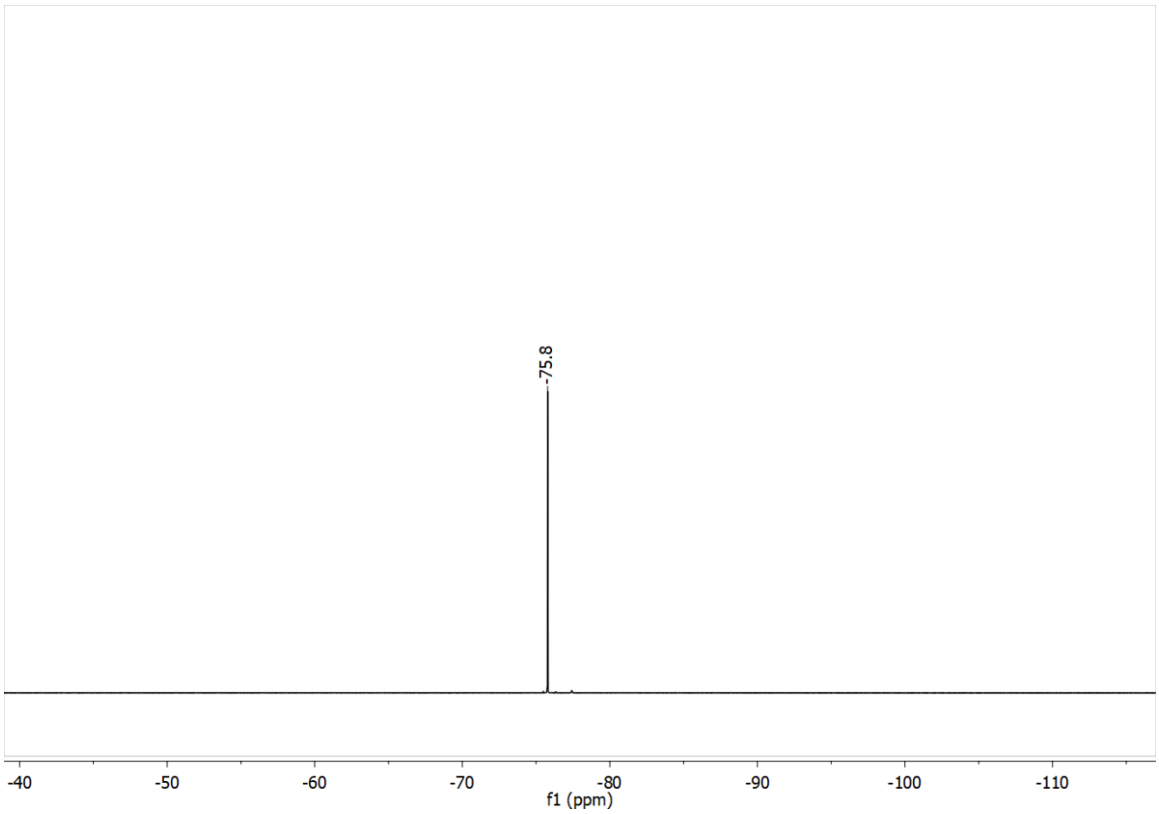

Figure S10. ^{19}F NMR spectrum of (^{Me}IPrCH)Si(Me)OTf{Si(SiMe$_3$)$_3$} (**3**) in C_6D_6.

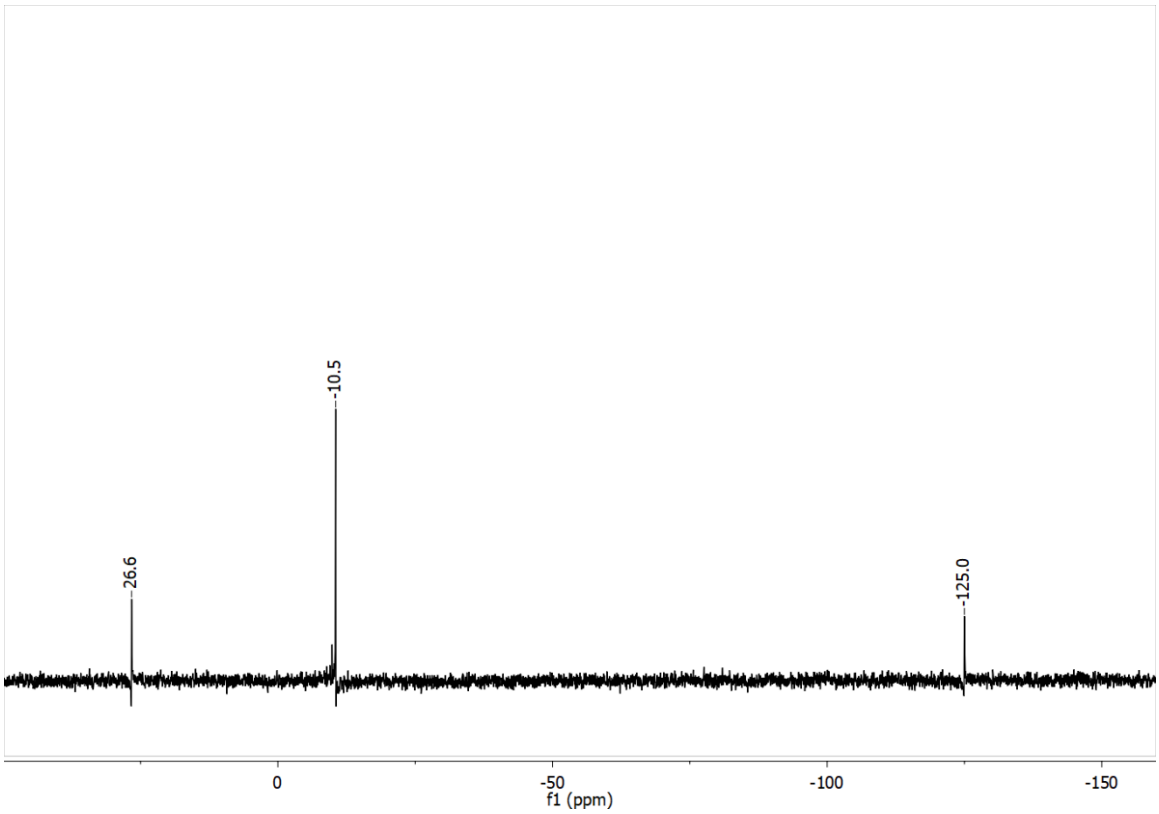

Figure S11. $^{29}Si\{^{1}H\}$ DEPT NMR spectrum of (^{Me}IPrCH)Si(Me)OTf{Si(SiMe$_3$)$_3$} (**3**) in C_6D_6 optimized for 7 Hz scalar coupling (3 adjacent proton).

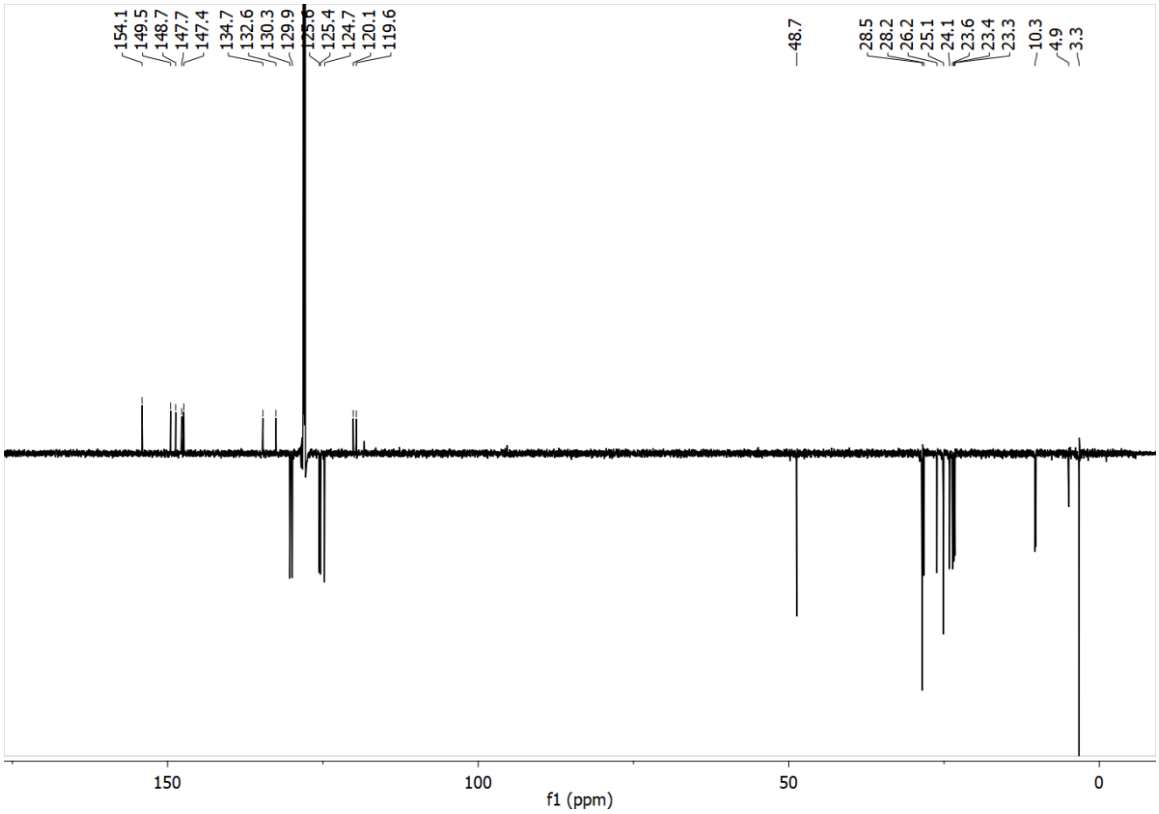

Figure S12. $^{13}C\{^{1}H\}$ DEPT NMR spectrum of (^{Me}IPrCH)Si(Me)OTf{Si(SiMe$_3$)$_3$} (**3**) in C_6D_6.

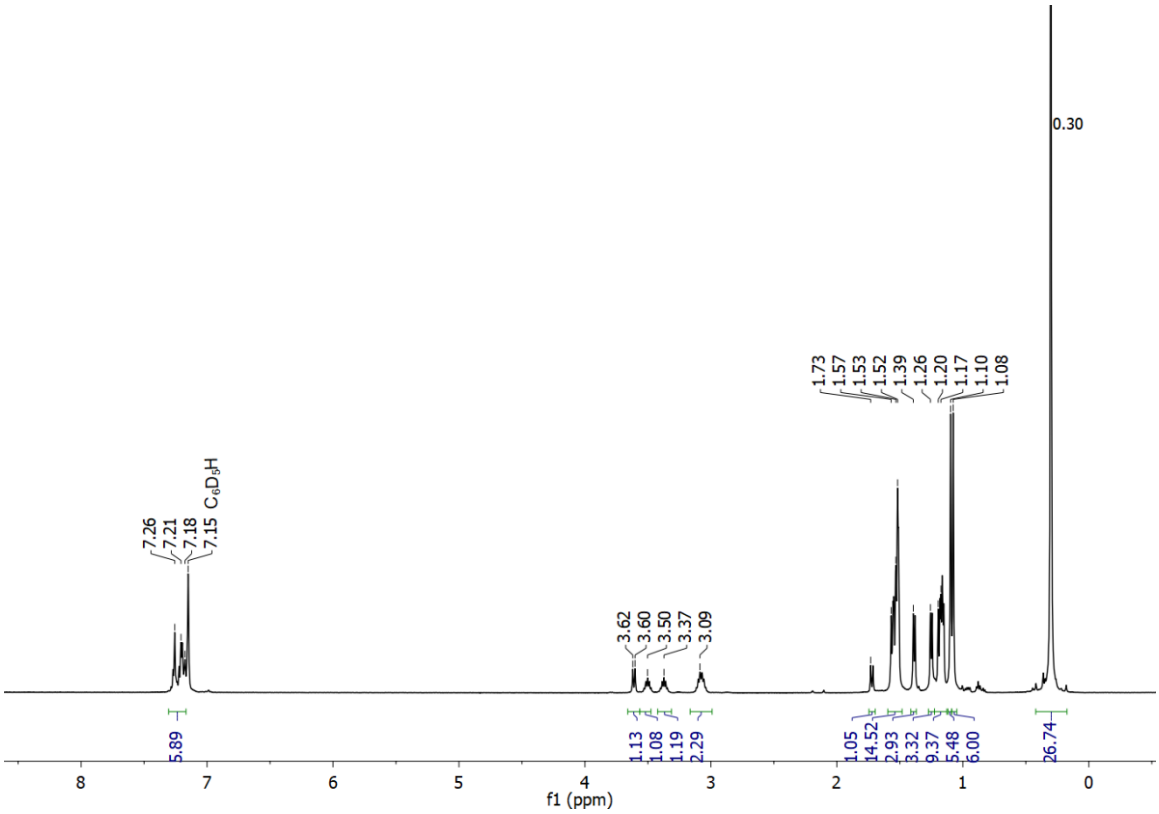

Figure S13. ^{1}H NMR spectrum of (^{Me}IPrCH)HSi(Bpin){Si(SiMe$_3$)$_3$} (**4**) in C_6D_6.

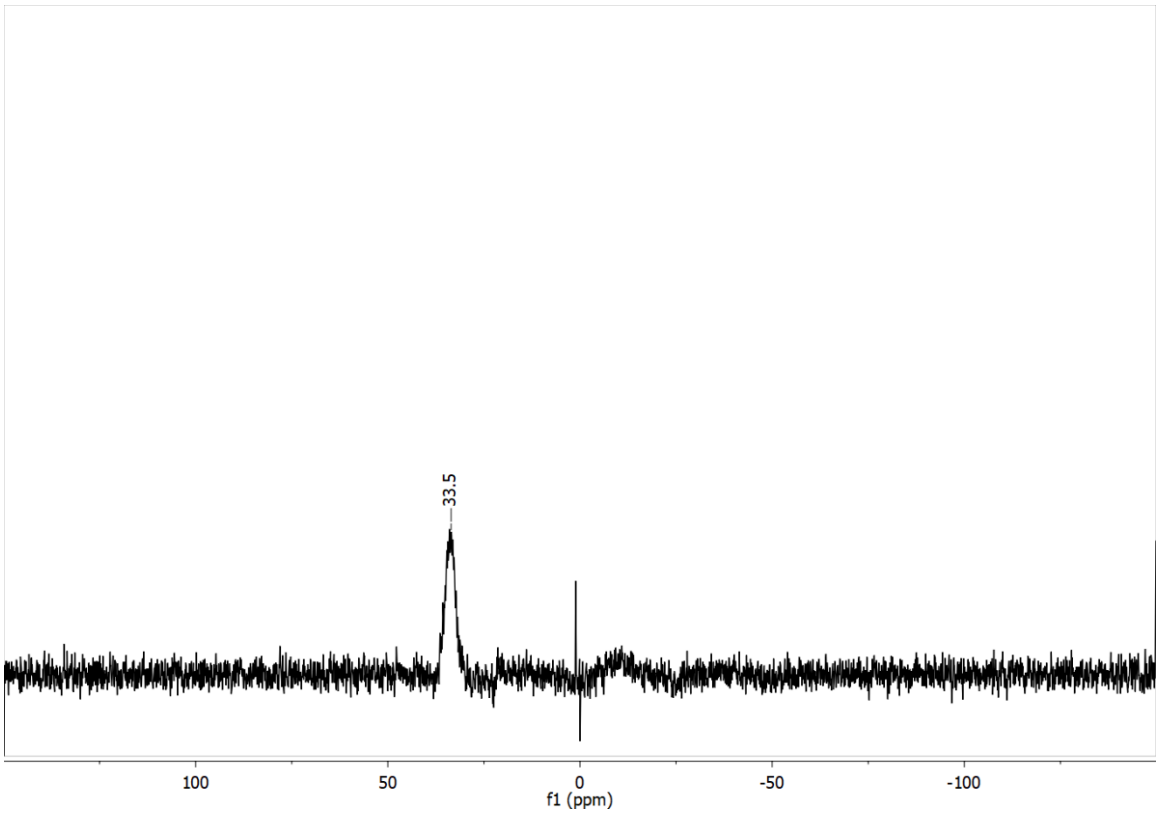

Figure S14. $^{11}B\{^{1}H\}$ NMR spectrum of (^{Me}IPrCH)HSi(Bpin){Si(SiMe$_3$)$_3$} (**4**) in C_6D_6.

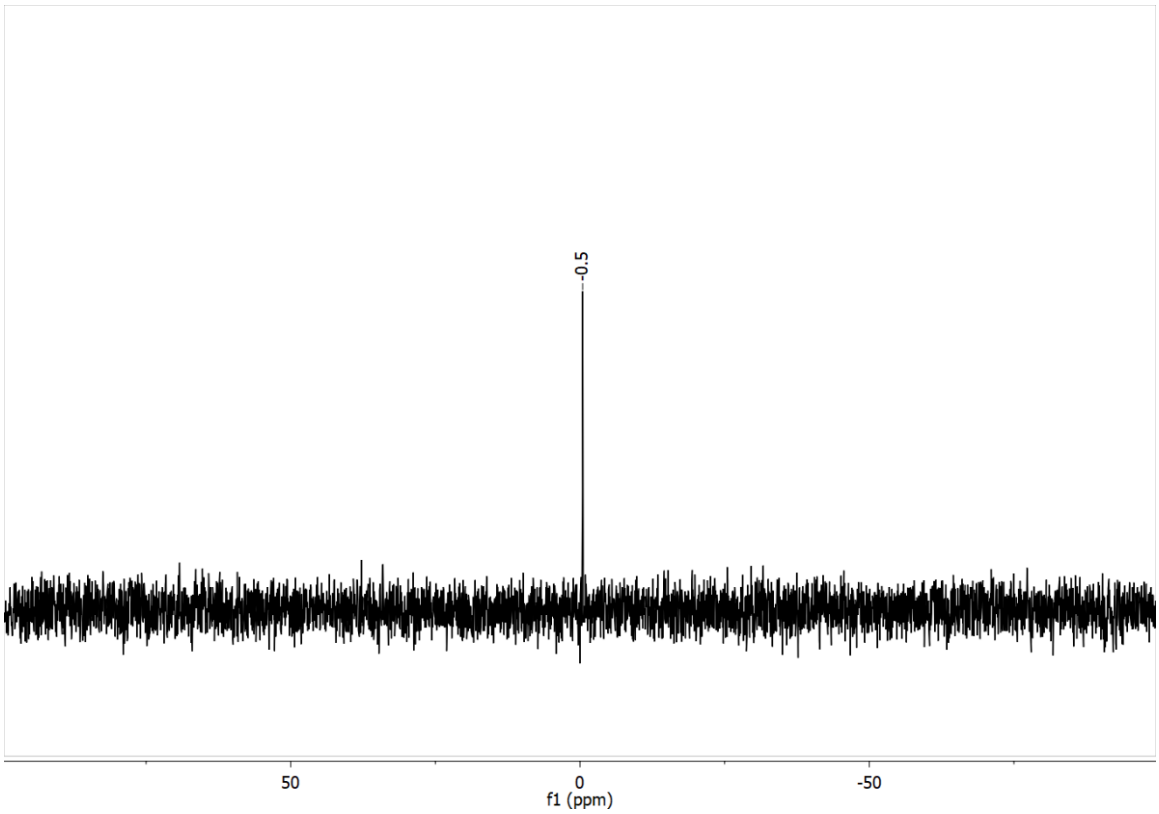

Figure S15. $^{29}Si\{^{1}H\}$ DEPT NMR spectrum of (^{Me}IPrCH)HSi(Bpin){Si(SiMe$_3$)$_3$} (**4**) in C_6D_6 optimized for 183 Hz scalar coupling (1 adjacent proton).

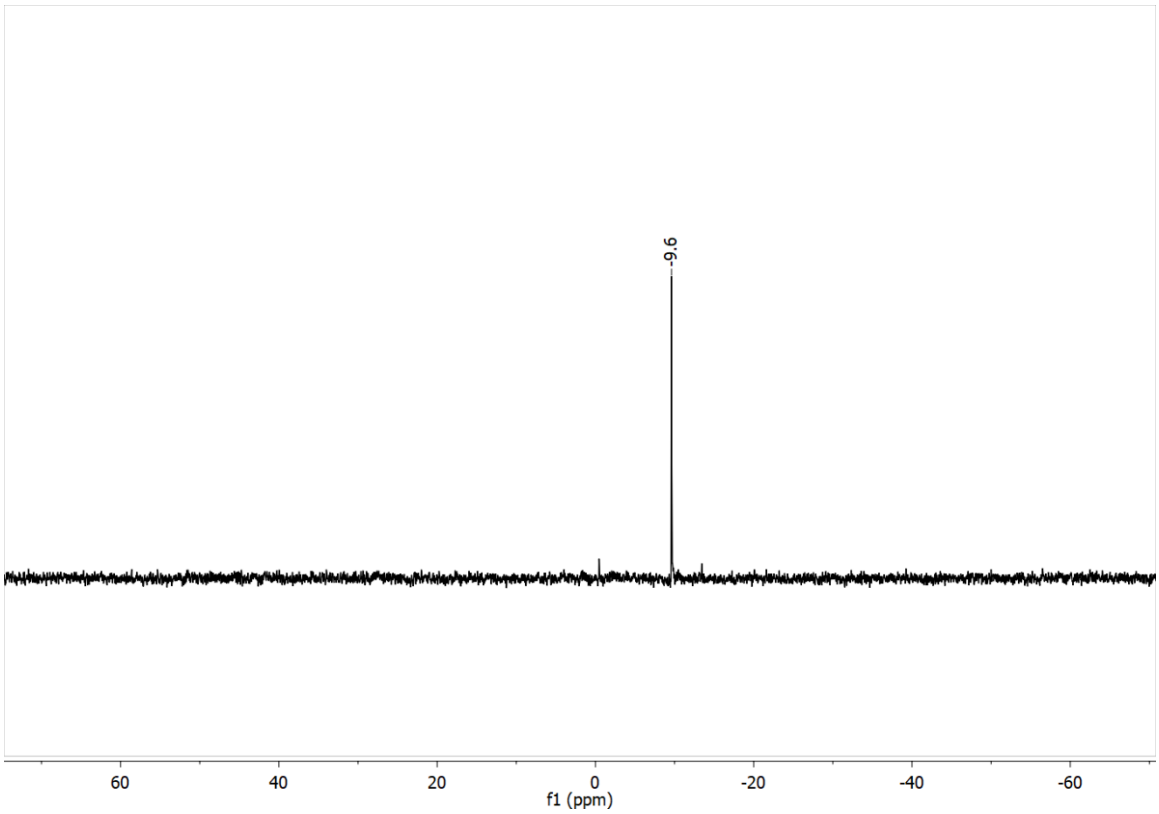

Figure S16. $^{29}Si\{^{1}H\}$ DEPT NMR spectrum of (^{Me}IPrCH)HSi(Bpin){Si(SiMe$_3$)$_3$} (**4**) in C_6D_6 optimized for 7 Hz scalar coupling (9 adjacent protons).

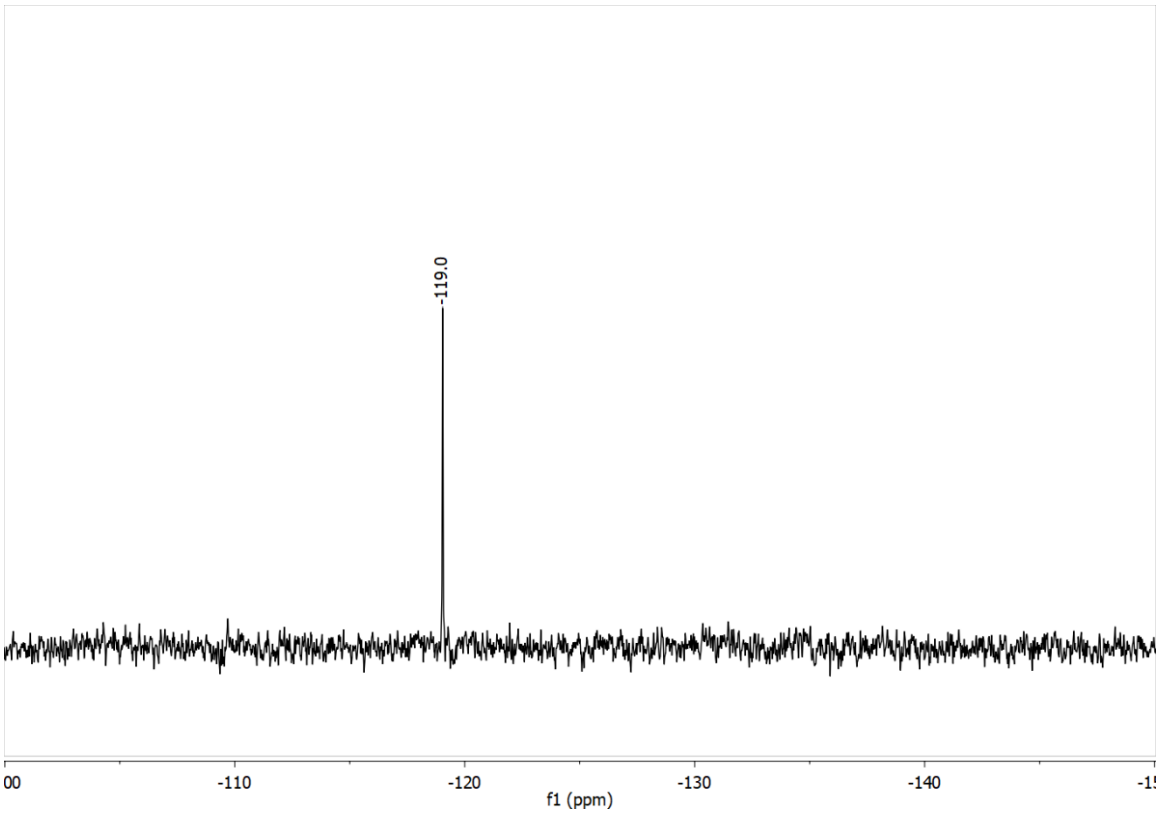

Figure S17. $^{29}Si\{^{1}H\}$ DEPT NMR spectrum of (^{Me}IPrCH)HSi(Bpin){Si(SiMe$_3$)$_3$} (**4**) in C_6D_6 optimized for 7 Hz scalar coupling (9 adjacent protons).

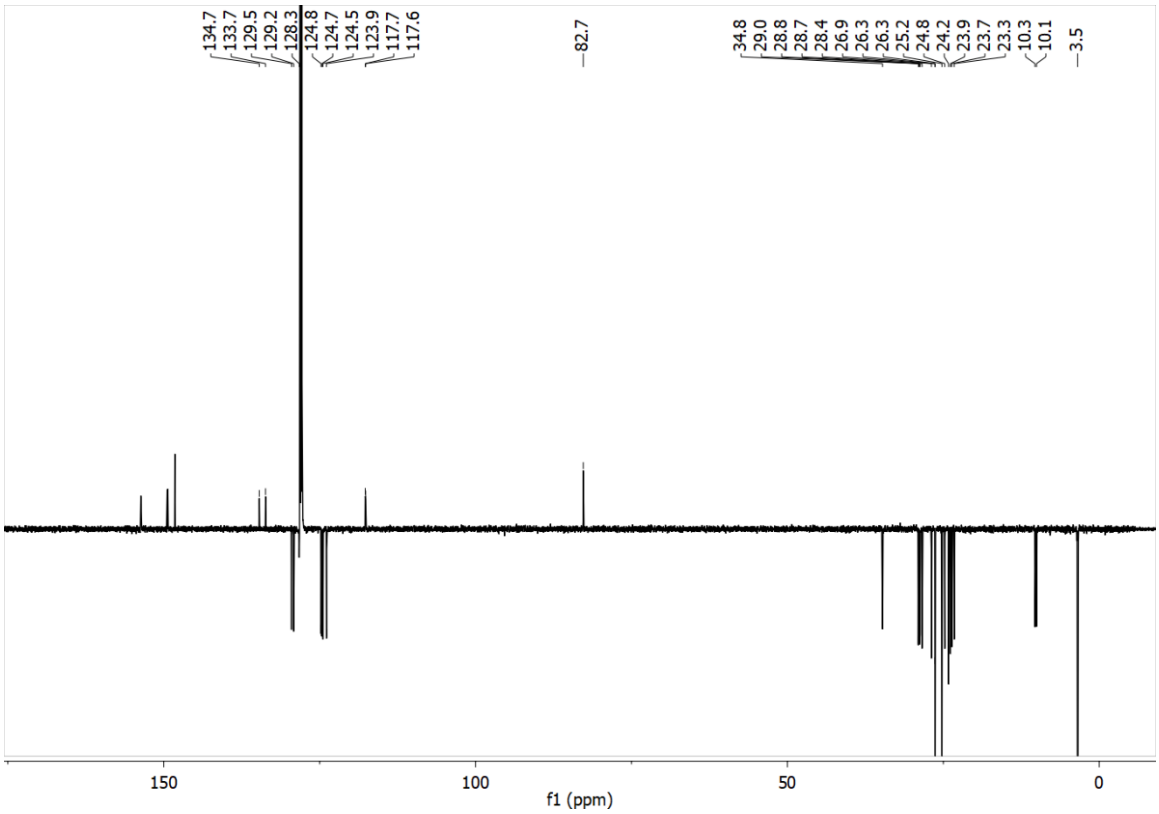

Figure S18. $^{13}C\{^{1}H\}$ DEPT NMR spectrum of (^{Me}IPrCH)HSi(Bpin){Si(SiMe$_3$)$_3$} (**4**) in C_6D_6.

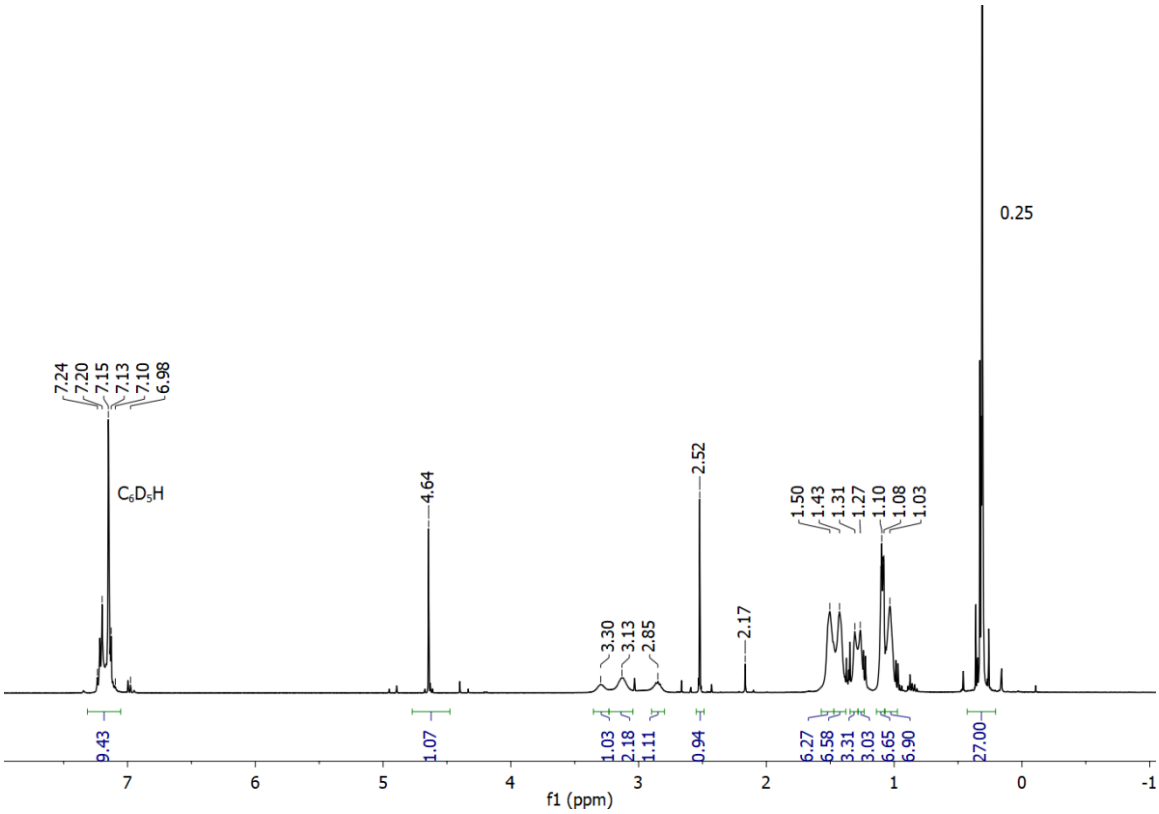

Figure S19. ^{1}H NMR spectrum of (^{Me}IPrCH)ClSi(HSiCl$_2$){Si(SiMe$_3$)$_3$} (**5**) in C_6D_6 at room temperature.

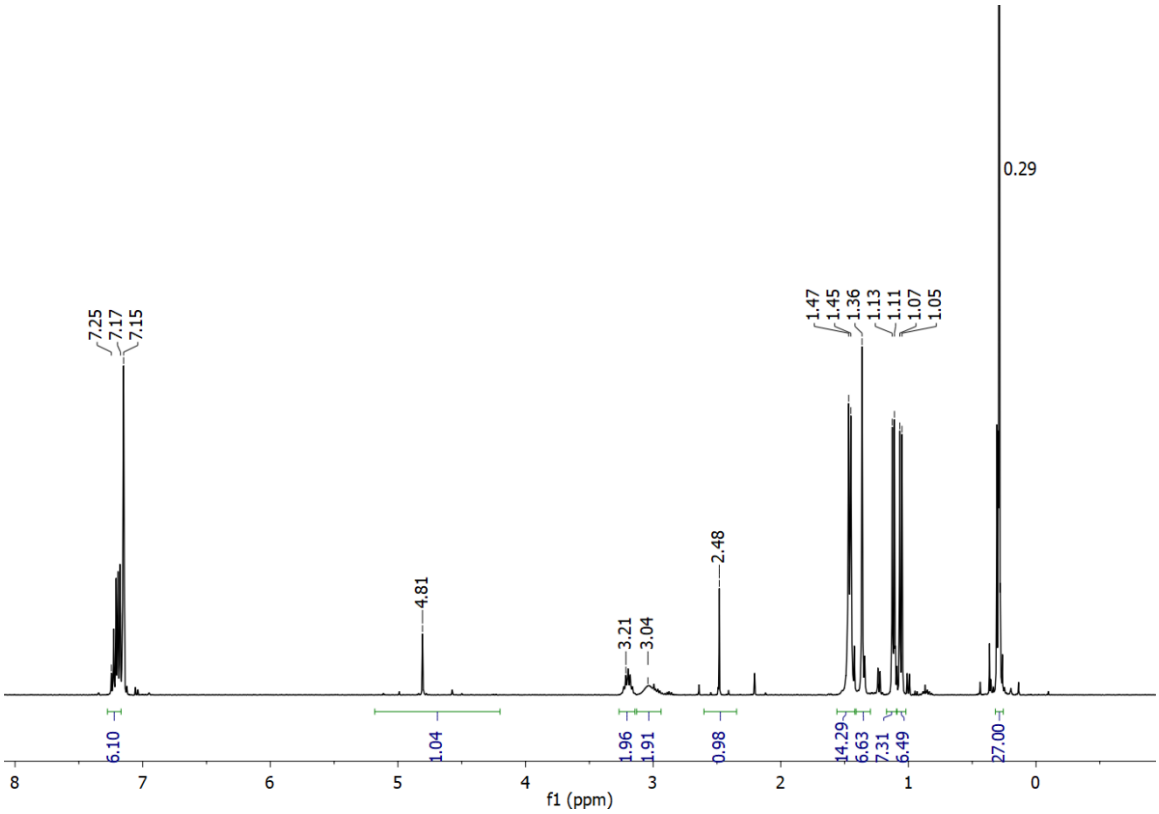

Figure S20. ^{1}H NMR spectrum of (^{Me}IPrCH)ClSi(HSiCl$_2$){Si(SiMe$_3$)$_3$} (**5**) in C_6D_6 at +75 °C.

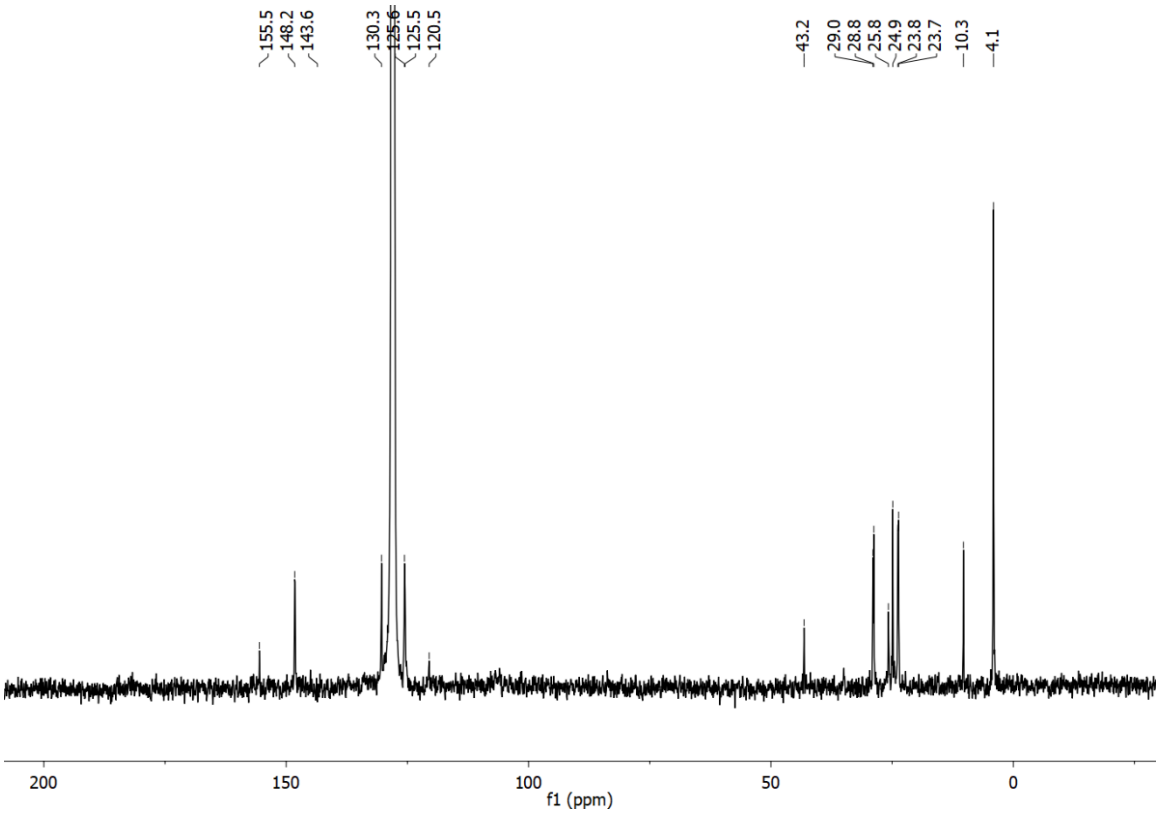

Figure S21. $^{13}C\{^{1}H\}$ NMR spectrum of (^{Me}IPrCH)ClSi(HSiCl$_2$){Si(SiMe$_3$)$_3$} (**5**) in C_6D_6 at +75 °C.

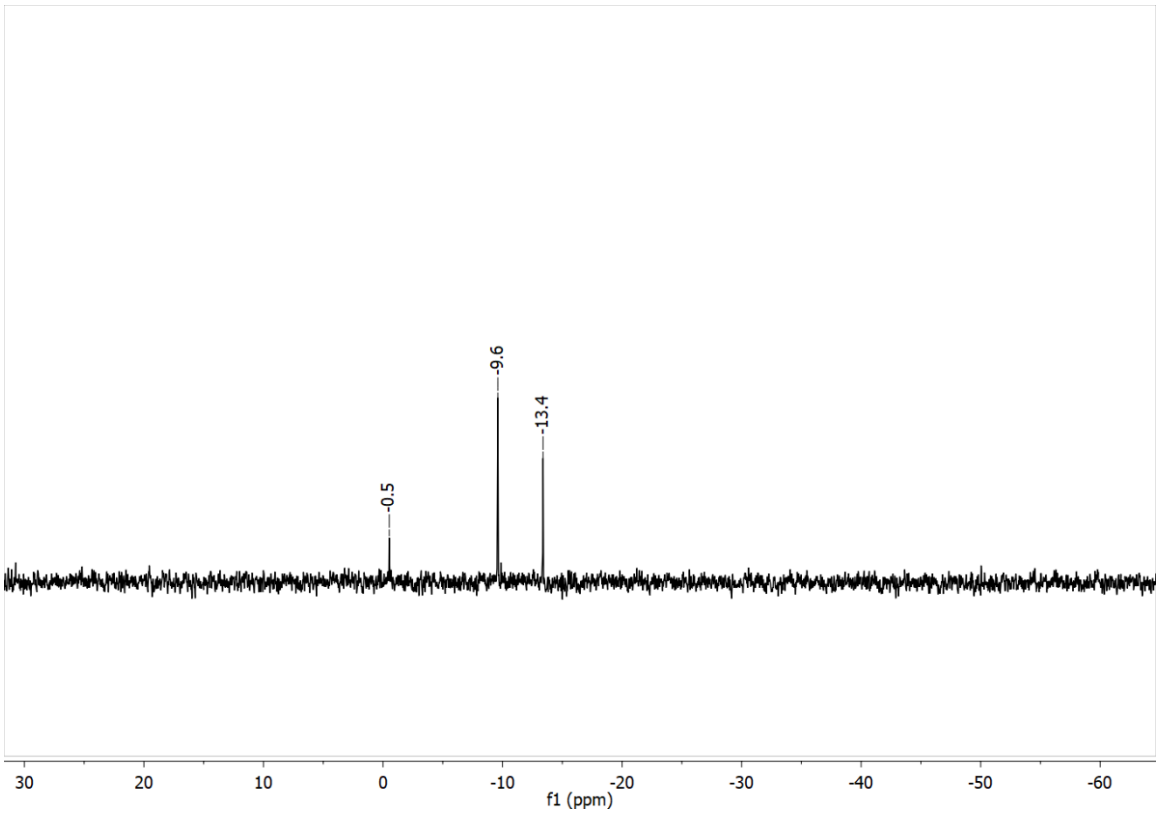

Figure S22. $^{29}Si\{^{1}H\}$ DEPT NMR spectrum of (^{Me}IPrCH)ClSi(HSiCl$_2$){Si(SiMe$_3$)$_3$} (**5**) in C_6D_6 at room temperature optimized for 24 Hz scalar coupling (1 adjacent proton).

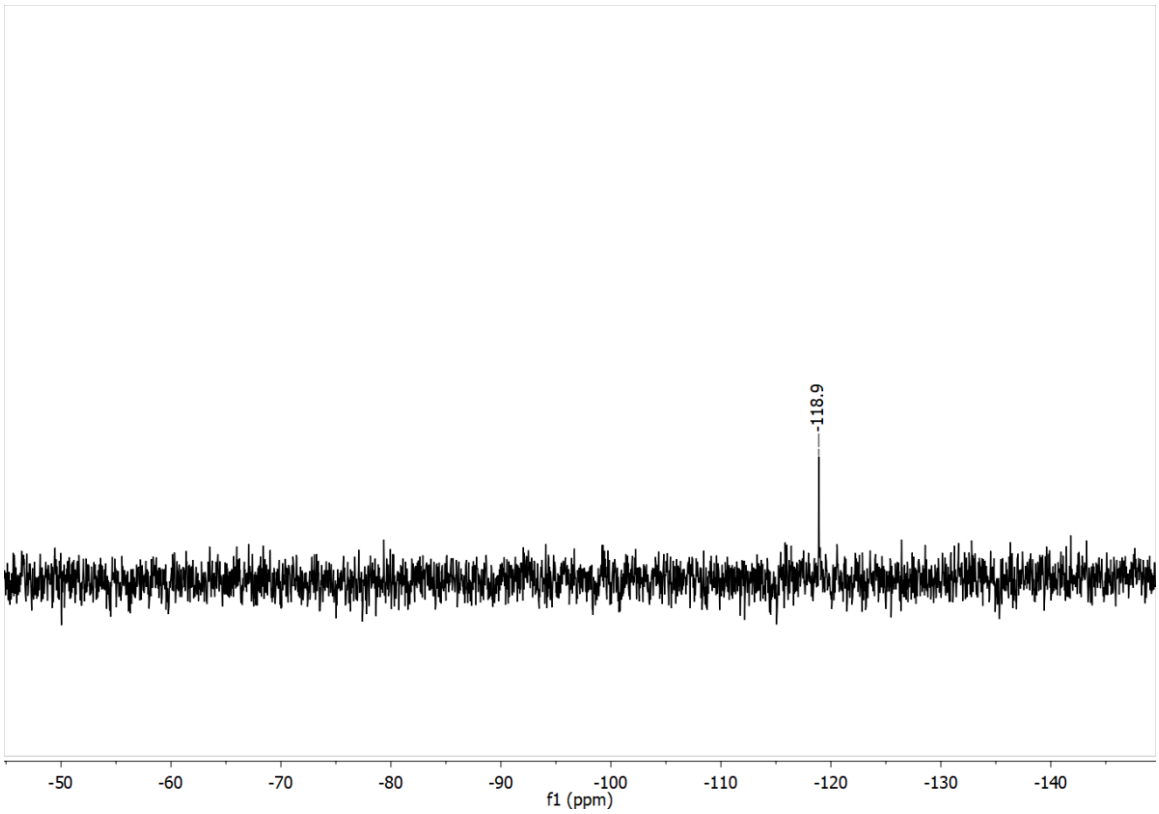

Figure S23. $^{29}Si\{^{1}H\}$ DEPT NMR spectrum of (^{Me}IPrCH)ClSi(HSiCl$_2$){Si(SiMe$_3$)$_3$} (**5**) in C_6D_6 at room temperature optimized for 7 Hz scalar coupling (9 adjacent protons).

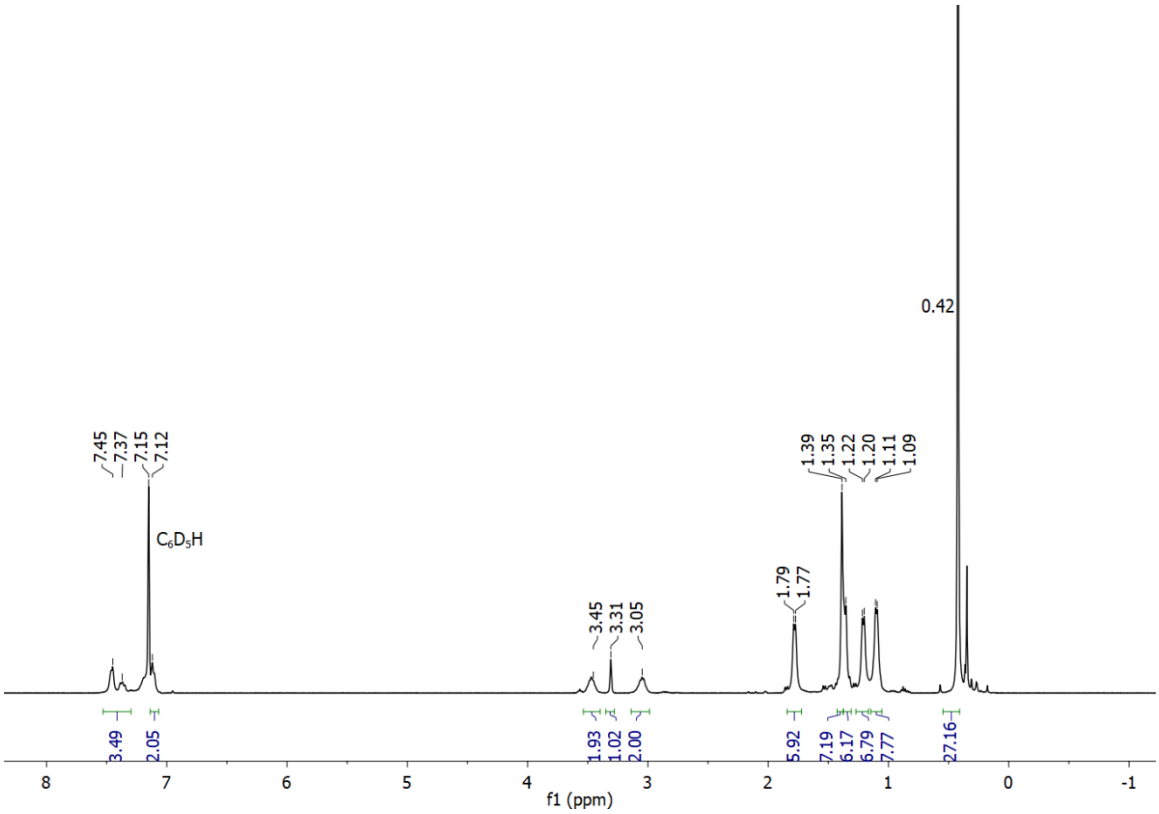

Figure S24. ^{1}H NMR spectrum of (^{Me}IPrCH)Si(P$_4$){Si(SiMe$_3$)$_3$} (**6**) in C$_6$D$_6$.

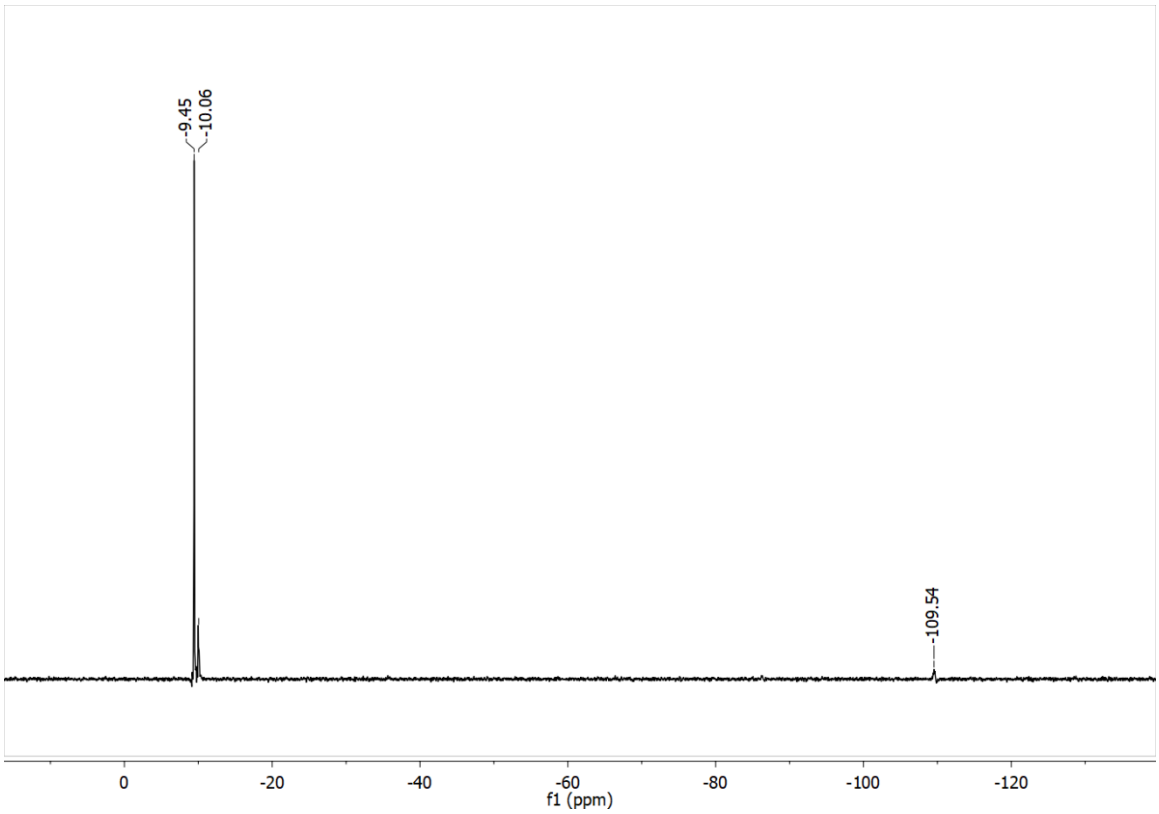

Figure S25. $^{29}Si\{^{1}H\}$ DEPT NMR spectrum of (^{Me}IPrCH)Si(P_4){Si($SiMe_3$)$_3$} (**6**) in C_6D_6 optimized for 7 Hz scalar coupling (9 adjacent protons).

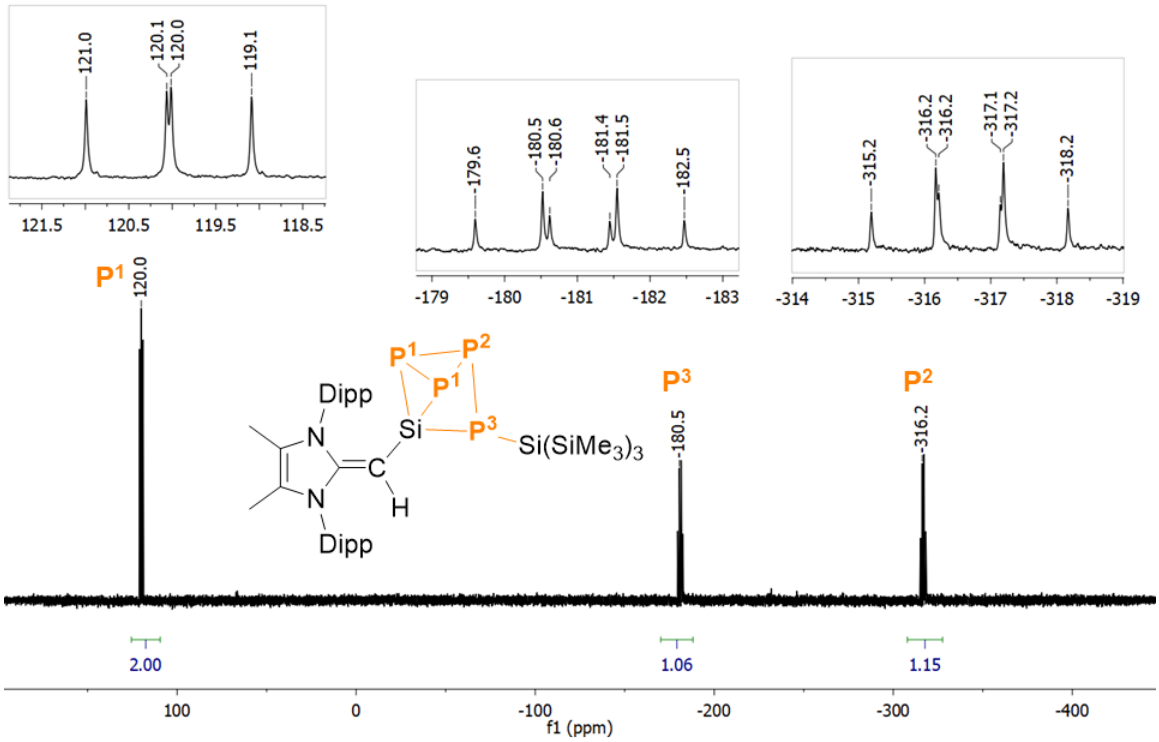

Figure S26. $^{31}P\{^{1}H\}$ NMR spectrum of (^{Me}IPrCH)Si(P_4){Si($SiMe_3$)$_3$} (**6**) in C_6D_6.

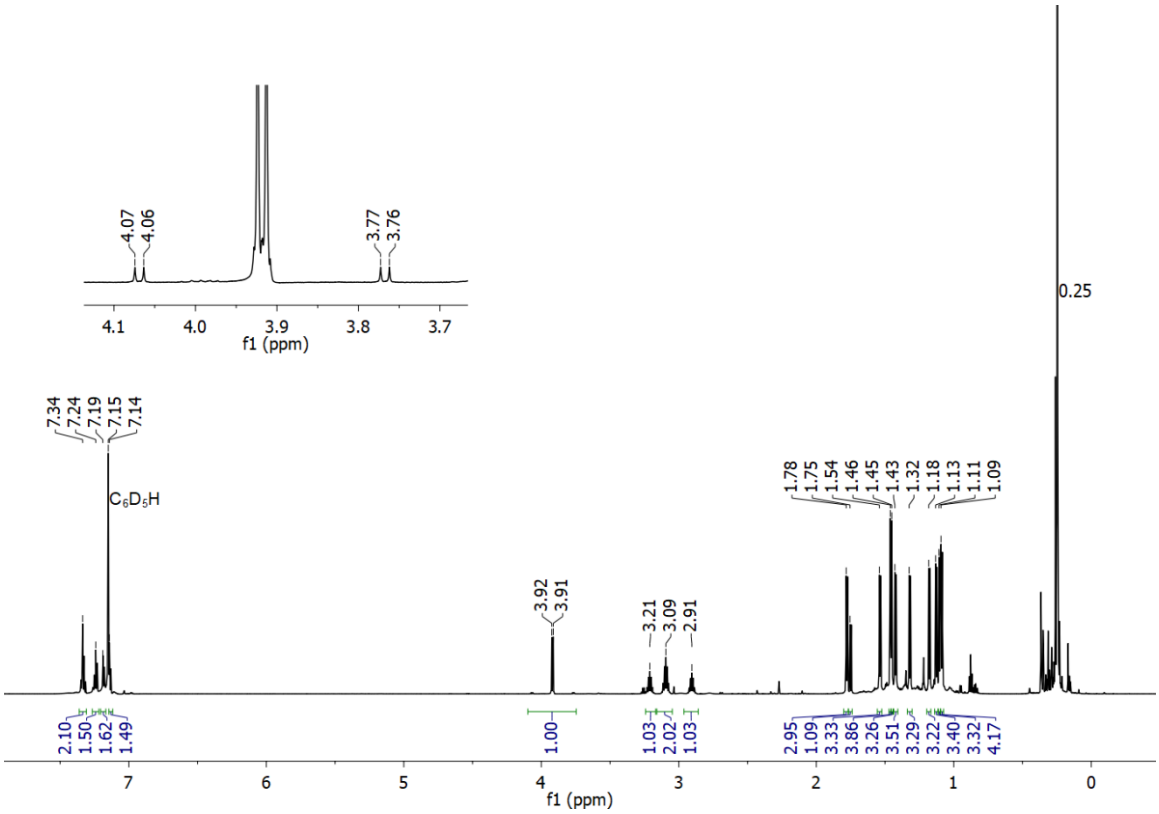

Figure S27. ^{1}H NMR spectrum of (^{Me}IPrCH)HSi(CN){Si(SiMe$_3$)$_3$} (**7**) in C_6D_6.

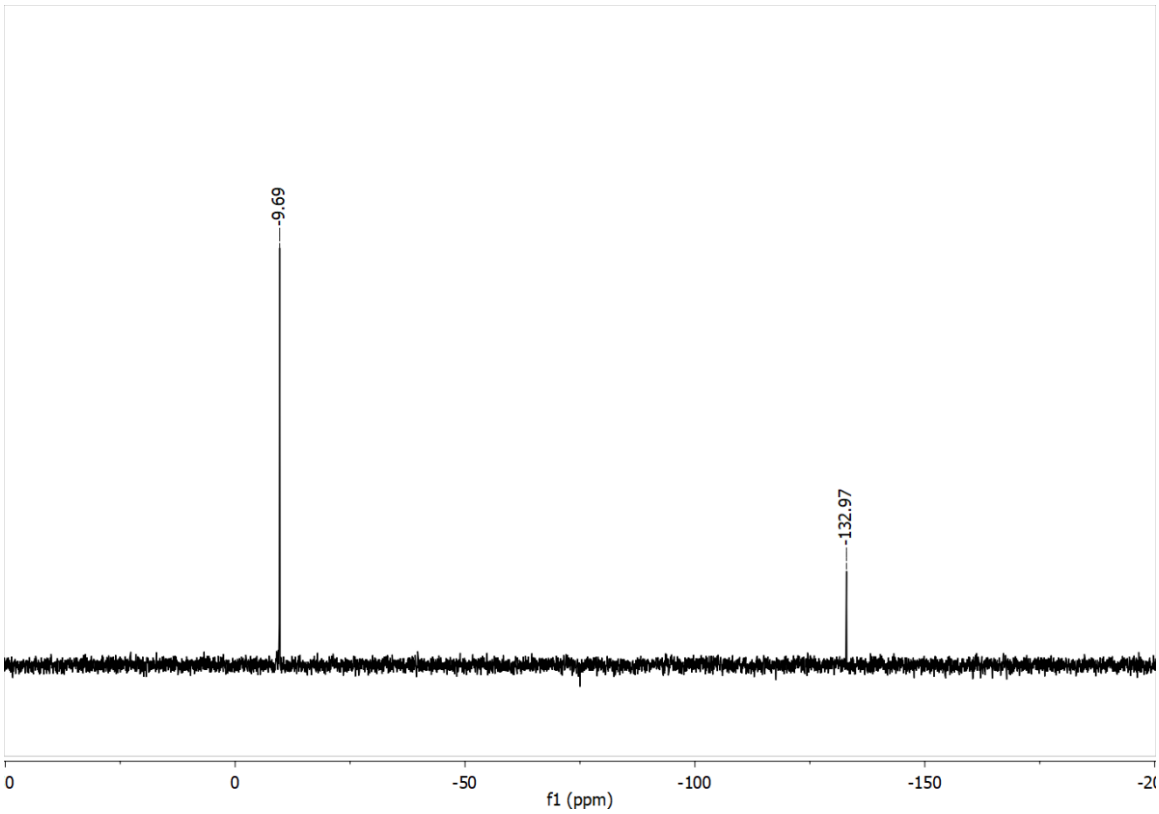

Figure S28. $^{29}Si\{^{1}H\}$ DEPT NMR spectrum of (^{Me}IPrCH)HSi(CN){Si(SiMe$_3$)$_3$} (**7**) in C_6D_6 optimized for 7 Hz scalar coupling (7 adjacent protons).

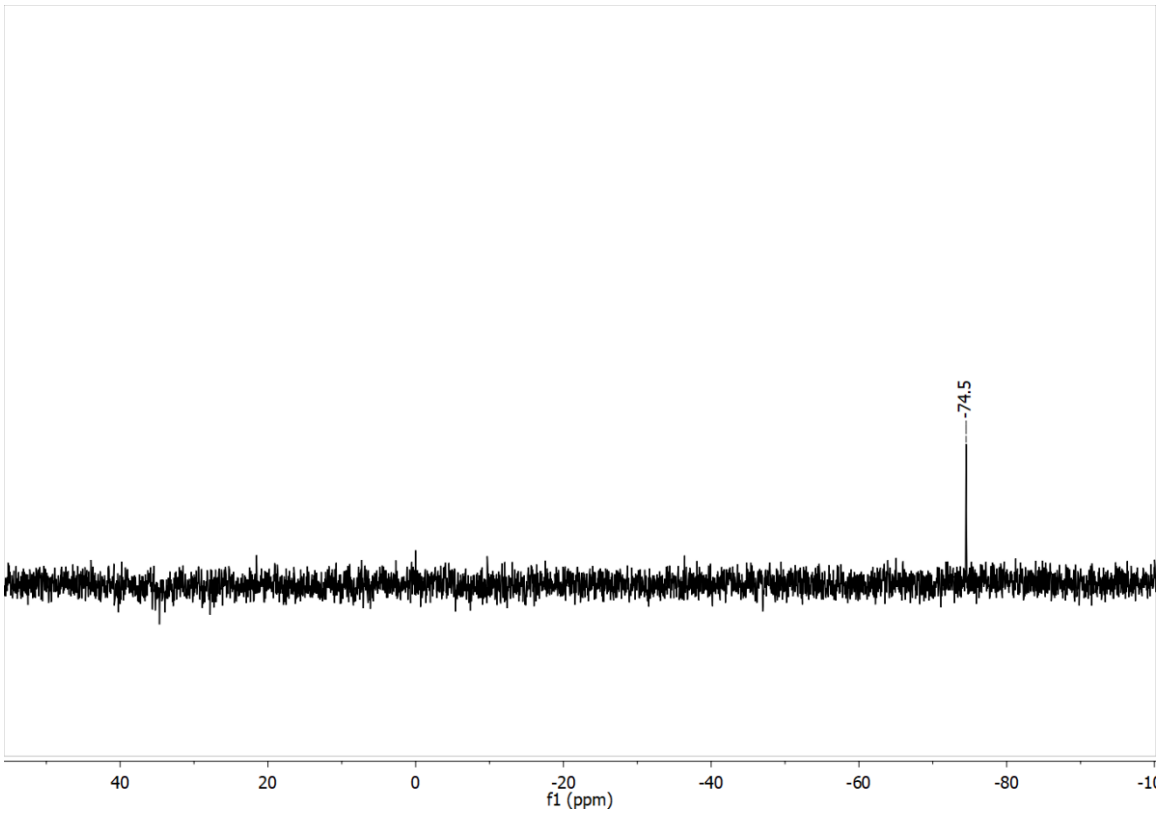

Figure S29. $^{29}Si\{^{1}H\}$ DEPT NMR spectrum of (^{Me}IPrCH)HSi(CN){Si(SiMe$_3$)$_3$} (**7**) in C_6D_6 optimized for 210 Hz scalar coupling (1 adjacent proton).

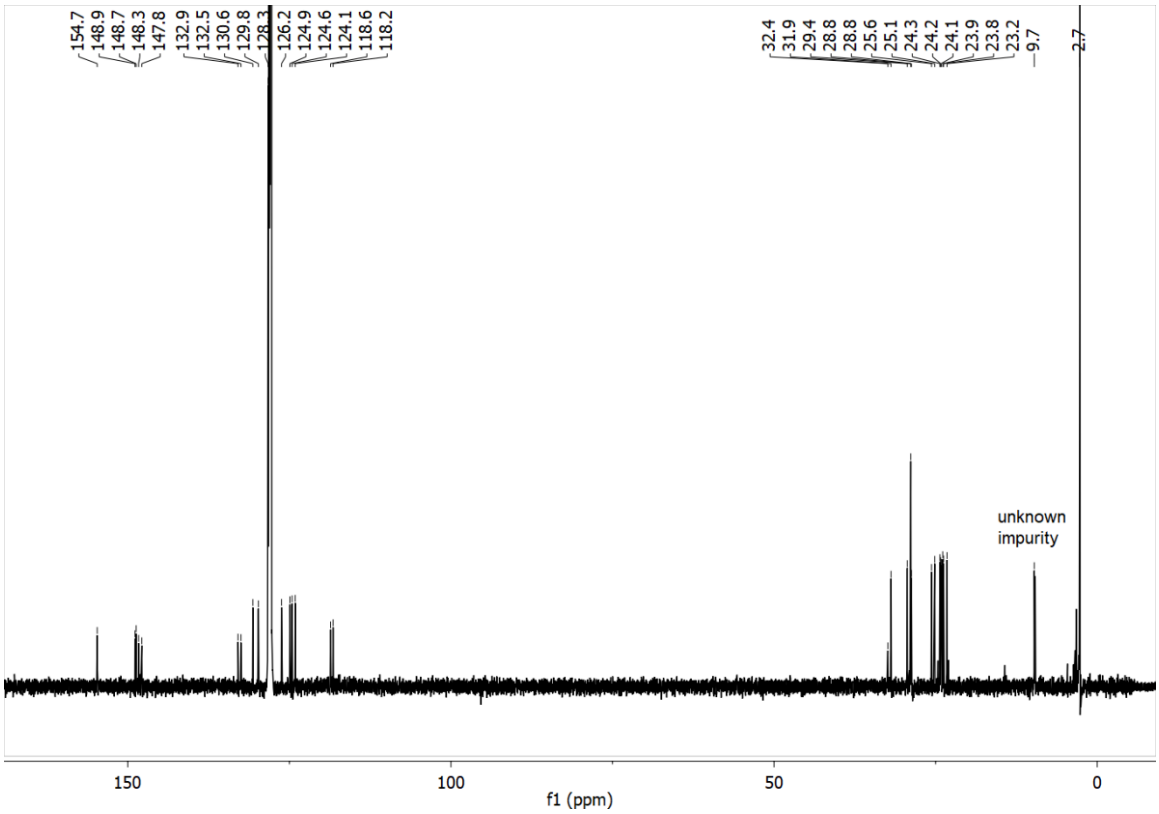

Figure S30. $^{13}C\{^{1}H\}$ NMR spectrum of (^{Me}IPrCH)HSi(CN){Si(SiMe$_3$)$_3$} (**7**) in C_6D_6.

X-Ray Crystallographic Data

Table S1. Crystallographic Details for (^{Me}IPrCH)SiBr$_3$ (**1**).

A. Crystal Data	
formula	$C_{30}H_{41}Br_3N_2Si$
formula weight	697.47
crystal dimensions (mm)	$0.23 \times 0.19 \times 0.07$
crystal system	triclinic
space group	$P\bar{1}$ (No. 2)
unit cell parameters[a]	
a (Å)	9.33020(15)
b (Å)	9.63981(15)
c (Å)	19.2808(3)
α (deg)	87.0024(11)
β (deg)	88.5252(12)
γ (deg)	67.0902(10)
V (Å^3)	1595.14(4)
Z	2
ρ_{calcd} (g cm^{-3})	1.452
μ (mm^{-1})	5.196
B. Data Collection and Refinement Conditions	
diffractometer	Bruker D8/APEX II CCD[b]
radiation (λ [Å])	Cu Kα (1.54178) (microfocus source)
temperature (°C)	–100
scan type	ω and ϕ scans (1.0°) (5 s exposures)
data collection 2θ limit (deg)	147.95
total data collected	10816 ($-11 \le h \le 11$, $-11 \le k \le 11$, $-24 \le l \le 23$)
independent reflections	6159 (R_{int} = 0.0657)
number of observed reflections (*NO*)	4408 [$F_o^2 \ge 2\sigma(F_o^2)$]
structure solution method	intrinsic phasing (*SHELXT-2014*[c])
refinement method	full-matrix least-squares on F^2 (*SHELXL–2014*[d])
absorption correction method	Gaussian integration (face-indexed)
range of transmission factors	0.8557–0.4583
data/restraints/parameters	6159 / 0 / 327
goodness-of-fit (S)[e] [all data]	0.974
final R indices[f]	
R_1 [$F_o^2 \ge 2\sigma(F_o^2)$]	0.0568
wR_2 [all data]	0.1584

largest difference peak and hole	1.042 and –1.417 e $Å^{-3}$

[a]Obtained from least-squares refinement of 8292 reflections with 4.58° < 2θ < 147.16°.

[b]Programs for diffractometer operation, data collection, data reduction and absorption correction were those supplied by Bruker.

[c] G. M. Sheldrick *Acta Crystallogr.* 2015, **A71**, 3–8.

[d] G. M. Sheldrick *Acta Crystallogr.* 2015, **C71**, 3–8.

[e]$S = [\Sigma w(F_o^2 - F_c^2)^2/(n - p)]^{1/2}$ (n = number of data; p = number of parameters varied; $w = [\sigma^2(F_o^2) + (0.0864P)^2]^{-1}$ where $P = [\mathrm{Max}(F_o^2, 0) + 2F_c^2]/3$).

[f]$R_1 = \Sigma||F_o| - |F_c||/\Sigma|F_o|$; $wR_2 = [\Sigma w(F_o^2 - F_c^2)^2/\Sigma w(F_o^4)]^{1/2}$.

Table S2. Crystallographic Details for (^{Me}IPrCH)Si{Si(SiMe$_3$)$_3$} (**2**).

A. Crystal Data	
formula	$C_{39}H_{68}N_2Si_5$
formula weight	705.40
crystal dimensions (mm)	0.36 × 0.30 × 0.15
crystal system	triclinic
space group	$P\bar{1}$ (No. 2)
unit cell parameters[a]	
a (Å)	10.3993(7)
b (Å)	12.5264(7)
c (Å)	18.4455(11)
α (deg)	88.449(3)
β (deg)	85.965(4)
γ (deg)	75.290(3)
V (Å^3)	2318.2(2)
Z	2
ρ_{calcd} (g cm^{-3})	1.011
μ (mm^{-1})	1.617
B. Data Collection and Refinement Conditions	
diffractometer	Bruker D8[b]
radiation (λ [Å])	Cu Kα (1.54178) (microfocus source)
temperature (°C)	–100
scan type	ω and ϕ scans (1.0°) (5 s exposures)[c]
data collection 2θ limit (deg)	148.31
total data collected	94354 (-12 ≤ h ≤ 0, -15 ≤ k ≤ 15, -22 ≤ l ≤ 22)
independent reflections	9029 (R_{int} = 0.0804)
number of observed reflections (*NO*)	7429 [$F_o^2 \geq 2\sigma(F_o^2)$]
structure solution method	intrinsic phasing (*SHELXT-2014*[c])
refinement method	full-matrix least-squares on F^2 (*SHELXL–2016*[d.])
absorption correction method	multi-scan (*SADABS*)
range of transmission factors	0.7823–0.4980
data/restraints/parameters	9029 / 0 / 434
goodness-of-fit (S)[e] [all data]	1.159
final R indices[f]	
R_1 [$F_o^2 \geq 2\sigma(F_o^2)$]	0.0526
wR_2 [all data]	0.1667
largest difference peak and hole	0.504 and –0.609 e Å^{-3}

[a]Obtained from least-squares refinement of 9924 reflections with 7.30° < 2θ <

147.16°.

[b]Programs for diffractometer operation, data collection, data reduction and absorption correction were those supplied by Bruker.

[c]G. M. Sheldrick *Acta Crystallogr.* 2015, **A71**, 3–8. (*SHELXT-2014*)

[d] G. M. Sheldrick *Acta Crystallogr.* 2015, **C71**, 3–8. (*SHELXL-2016*)

[e]$S = [\Sigma w(F_o^2 - F_c^2)^2/(n - p)]^{1/2}$ (n = number of data; p = number of parameters varied; $w = [\sigma^2(F_o^2) + (0.0773P)^2 + 1.1780P]^{-1}$ where $P = [\mathrm{Max}(F_o^2, 0) + 2F_c^2]/3$).

[f]$R_1 = \Sigma||F_o| - |F_c||/\Sigma|F_o|$; $wR_2 = [\Sigma w(F_o^2 - F_c^2)^2/\Sigma w(F_o^4)]^{1/2}$.

Table S3. Crystallographic Details for (^{Me}IPrCH)Si(Me)OTf{Si(SiMe$_3$)$_3$} (**3**).

A. Crystal Data	
formula	$C_{41}H_{71}F_3N_2O_3SSi_5$
formula weight	869.50
crystal dimensions (mm)	0.45 × 0.31 × 0.25
crystal system	monoclinic
space group	$P2_1/c$ (No. 14)
unit cell parameters[a]	
a (Å)	20.6562(5)
b (Å)	13.3097(3)
c (Å)	19.8440(5)
β (deg)	109.6576(9)
V (Å^3)	5137.7(2)
Z	4
ρ_{calcd} (g cm^{-3})	1.124
μ (mm^{-1})	2.048
B. Data Collection and Refinement Conditions	
diffractometer	Bruker D8/APEX II CCD[b]
radiation (λ [Å])	Cu Kα (1.54178) (microfocus source)
temperature (°C)	–100
scan type	ω and ϕ scans (1.0°) (5 s exposures)
data collection 2θ limit (deg)	148.39
total data collected	240012 (-25 ≤ h ≤ 25, -16 ≤ k ≤ 16, -24 ≤ l ≤ 23)
independent reflections	10457 (R_{int} = 0.0371)
number of observed reflections (*NO*)	0.0371 [$F_o^2 \geq 2\sigma(F_o^2)$]
structure solution method	intrinsic phasing (*SHELXT-2014*[c])
refinement method	full-matrix least-squares on F^2 (*SHELXL–2017*[d])
absorption correction method	Gaussian integration (face-indexed)
range of transmission factors	0.7327–0.5467
data/restraints/parameters	10457 / 0 / 546
goodness-of-fit (S)[e] [all data]	1.032
final R indices[f]	
R_1 [$F_o^2 \geq 2\sigma(F_o^2)$]	0.0319
wR_2 [all data]	0.0932
largest difference peak and hole	0.300 and –0.435 e Å^{-3}

[a]Obtained from least-squares refinement of 9640 reflections with 8.04° < 2θ < 147.72°.

[b]Programs for diffractometer operation, data collection, data reduction and absorption correction were those supplied by Bruker.

[c] G. M. Sheldrick *Acta Crystallogr.* 2015, **A71**, 3–8. (*SHELXT-2014*)

[d] G. M. Sheldrick *Acta Crystallogr.* 2015, **C71**, 3–8. (*SHELXL-2017*)

[e] $S = [\Sigma w(F_o^2 - F_c^2)^2/(n - p)]^{1/2}$ (n = number of data; p = number of parameters varied; $w = [\sigma^2(F_o^2) + (0.0489P)^2 + 1.8701P]^{-1}$ where $P = [\mathrm{Max}(F_o^2, 0) + 2F_c^2]/3$).

[f] $R_1 = \Sigma||F_o| - |F_c||/\Sigma|F_o|$; $wR_2 = [\Sigma w(F_o^2 - F_c^2)^2/\Sigma w(F_o^4)]^{1/2}$.

Table S4. Crystallographic Details for (^{Me}IPrCH)SiCl(HSiCl$_2$){Si(SiMe$_3$)$_3$} (**5**).

A. Crystal Data	
formula	$C_{39}H_{69}Cl_3N_2Si_6$
formula weight	840.85
crystal dimensions (mm)	0.32 × 0.08 × 0.03
crystal system	monoclinic
space group	$P2_1/n$ (an alternate setting of $P2_1/c$ [No. 14])
unit cell parameters[a]	
a (Å)	10.4358(6)
b (Å)	19.1606(5)
c (Å)	24.4753(8)
β (deg)	95.466(3)
V (Å^3)	4871.7(3)
Z	4
ρ_{calcd} (g cm^{-3})	1.146
μ (mm^{-1})	3.320
B. Data Collection and Refinement Conditions	
diffractometer	Bruker D8/APEX II CCD[b]
radiation (λ [Å])	Cu Kα (1.54178) (microfocus source)
temperature (°C)	–100
scan type	ω and ϕ scans (1.0°) (5-10-15 s exposures)[c]
data collection 2θ limit (deg)	140.52
total data collected	10180 (-12 ≤ h ≤ 12, 0 ≤ k ≤ 23, 0 ≤ l ≤ 29)
independent reflections	10180 (R_{int} = 0.0934)
number of observed reflections (*NO*)	7477 [$F_o^2 \geq 2\sigma(F_o^2)$]
structure solution method	intrinsic phasing (*SHELXT-2014*[d])
refinement method	full-matrix least-squares on F^2 (*SHELXL–2017*[e])
absorption correction method	multi-scan (*TWINABS*)
range of transmission factors	0.7738–0.5282
data/restraints/parameters	10180 / 51[f] / 491
goodness-of-fit (S)[g] [all data]	1.032
final R indices[h]	
R_1 [$F_o^2 \geq 2\sigma(F_o^2)$]	0.0768
wR_2 [all data]	0.2177
largest difference peak and hole	0.891 and –0.589 e Å^{-3}

[a]Obtained from least-squares refinement of 6261 reflections with 7.26° < 2θ < 139.58°.

[b]Programs for diffractometer operation, data collection, data reduction and absorption correction were those supplied by Bruker. The crystal used for data collection was found to display non-merohedral twinning. Both components of the twin were indexed with the program *CELL_NOW* (Bruker AXS Inc., Madison, WI, 2004). The second twin component can be related to the first component by 180º rotation about the [1 0 0] axis in real space and about the [1 0 -0.227] axis in reciprocal space. Integrated intensities for the reflections from the two components were written into a *SHELXL-2014* HKLF 5 reflection file with the data integration program *SAINT* (version 8.38A), using all reflection data (exactly overlapped, partially overlapped and non-overlapped). The refined value of the twin fraction (*SHELXL-2014* BASF parameter) was 0.4636(17).

[c]Data were collected with the detector set at three different positions. Low-angle (detector 2θ = –33º) data frames were collected using a scan time of 5 s, medium-angle (detector 2θ = 75º) frames using a scan time of 10 s, and high-angle (detector 2θ = 117º) frames using a scan time of 15 s.

[d] G. M. Sheldrick *Acta Crystallogr.* 2015, **A71**, 3–8. (*SHELXT-2014*)

[e] G. M. Sheldrick *Acta Crystallogr.* 2015, **C71**, 3–8. (*SHELXL-2017*)

[f]The Si6–C distances of the disordered trimethylsilyl group were restrained to be approximately the same by use of the *SHELXL* **SADI** instruction (15 restraints). Additionally, the anisotropic displacement parameters for that group were restrained by use of the *SHELXL* **RIGU** instruction (36 restraints).

[g]$S = [\Sigma w(F_o^2 - F_c^2)^2/(n - p)]^{1/2}$ (n = number of data; p = number of parameters varied; $w = [\sigma^2(F_o^2) + (0.1072P)^2 + 6.7861P]^{-1}$ where $P = [\mathrm{Max}(F_o^2, 0) + 2F_c^2]/3$).

[h]$R_1 = \Sigma||F_o| - |F_c||/\Sigma|F_o|$; $wR_2 = [\Sigma w(F_o^2 - F_c^2)^2/\Sigma w(F_o^4)]^{1/2}$.

Table S5. Crystallographic Details for (^{Me}IPrCH)Si(P_4){Si($SiMe_3$)$_3$} (**6**).

A. Crystal Data	
formula	$C_{39}H_{64}N_2P_4Si_5$
formula weight	825.25
crystal dimensions (mm)	0.26 × 0.26 × 0.17
crystal system	triclinic
space group	$P\bar{1}$ (No. 2)
unit cell parameters[a]	
a (Å)	10.1314(4)
b (Å)	13.5879(6)
c (Å)	18.6001(7)
α (deg)	78.391(3)
β (deg)	85.188(2)
γ (deg)	77.406(3)
V (Å^3)	2445.70(17)
Z	2
ρ_{calcd} (g cm^{-3})	1.121
μ (mm^{-1})	2.802
B. Data Collection and Refinement Conditions	
diffractometer	Bruker D8[b]
radiation (λ [Å])	Cu Kα (1.54178) (microfocus source)
temperature (°C)	–100
scan type	ω and ϕ scans (1.0°) (5-10-15 s exposures)[c]
data collection 2θ limit (deg)	148.54
total data collected	17281 (-12≤ h ≤ 12, -16 ≤ k ≤ 16, -23 ≤ l ≤ 23)
independent reflections	9501 (R_{int} = 0.0390)
number of observed reflections (*NO*)	7735 [$F_o^2 \geq 2\sigma(F_o^2)$]
structure solution method	intrinsic phasing (*SHELXT-2014*[d])
refinement method	full-matrix least-squares on F^2 (*SHELXL–2016*[e])
absorption correction method	multi-scan (*SADABS*)
range of transmission factors	0.7537–0.7537
data/restraints/parameters	9501 / 0 / 470
goodness-of-fit (S)[f] [all data]	1.035
final R indices[g]	
R_1 [$F_o^2 \geq 2\sigma(F_o^2)$]	0.0603
wR_2 [all data]	0.1837
largest difference peak and hole	0.819 and –0.779 e Å^{-3}

[a]Obtained from least-squares refinement of 9833 reflections with 4.86° < 2θ < 146.80°.

[b]Programs for diffractometer operation, data collection, data reduction and absorption correction were those supplied by Bruker.

[c]Data were collected with the detector set at three different positions. Low-angle (detector 2θ = −33°) data frames were collected using a scan time of 5 s, medium-angle (detector 2θ = 75°) frames using a scan time of 10 s, and high-angle (detector 2θ = 117°) frames using a scan time of 15 s.

[d] G. M. Sheldrick *Acta Crystallogr.* 2015, **A71**, 3–8. (*SHELXT-2014*)

[e] G. M. Sheldrick *Acta Crystallogr.* 2015, **C71**, 3–8. (*SHELXL-2016*)

[f]$S = [\Sigma w(F_o^2 - F_c^2)^2/(n - p)]^{1/2}$ (n = number of data; p = number of parameters varied; $w = [\sigma^2(F_o^2) + (0.1025P)^2 + 1.8244P]^{-1}$ where $P = [\mathrm{Max}(F_o^2, 0) + 2F_c^2]/3$).

[g]$R_1 = \Sigma||F_o| - |F_c||/\Sigma|F_o|$; $wR_2 = [\Sigma w(F_o^2 - F_c^2)^2/\Sigma w(F_o^4)]^{1/2}$.

Table S6. Crystallographic Details for (^{Me}IPrCH)SiH(CN){Si(SiMe$_3$)$_3$} (**7**).

A. Crystal Data	
formula	$C_{40}H_{69}N_3Si_5$
formula weight	732.43
crystal dimensions (mm)	0.26 × 0.21 × 0.13
crystal system	monoclinic
space group	$P2_1/m$ (No. 11)
unit cell parameters[a]	
a (Å)	11.3610(2)
b (Å)	18.2937(4)
c (Å)	11.6759(2)
β (deg)	105.7582(8)
V (Å^3)	2335.46(8)
Z	2
ρ_{calcd} (g cm^{-3})	1.042
μ (mm^{-1})	1.628
B. Data Collection and Refinement Conditions	
diffractometer	Bruker D8/APEX II CCD[b]
radiation (λ [Å])	Cu Kα (1.54178) (microfocus source)
temperature (°C)	–100
scan type	ω and ϕ scans (1.0°) (5 s exposures)
data collection 2θ limit (deg)	148.57
total data collected	16666 (-14 ≤ h ≤ 14, -22 ≤ k ≤ 22, -14 ≤ l ≤ 14)
independent reflections	4908 (R_{int} = 0.0163)
number of observed reflections (*NO*)	4547 [$F_o^2 \geq 2\sigma(F_o^2)$]
structure solution method	intrinsic phasing (*SHELXT-2014*[c])
refinement method	full-matrix least-squares on F^2 (*SHELXL–2017*[d])
absorption correction method	Gaussian integration (face-indexed)
range of transmission factors	0.6649–0.5441
data/restraints/parameters	4908 / 0 / 325
goodness-of-fit (S)[e] [all data]	1.010
final R indices[f]	
R_1 [$F_o^2 \geq 2\sigma(F_o^2)$]	0.0786
wR_2 [all data]	0.2282
largest difference peak and hole	1.562 and –0.469 e Å^{-3}

[a]Obtained from least-squares refinement of 9889 reflections with 4.84° < 2θ < 147.54°.

[b]Programs for diffractometer operation, data collection, data reduction and absorption correction were those supplied by Bruker.

[c] G. M. Sheldrick *Acta Crystallogr.* 2015, **A71**, 3–8. (*SHELXT-2014*)

[d] G. M. Sheldrick *Acta Crystallogr.* 2015, **A71**, 3–8. (*SHELXL-2017*)

[e] $S = [\Sigma w(F_o^2 - F_c^2)^2/(n - p)]^{1/2}$ (n = number of data; p = number of parameters varied; $w = [\sigma^2(F_o^2) + (0.1303P)^2 + 2.0865P]^{-1}$ where $P = [\mathrm{Max}(F_o^2, 0) + 2F_c^2]/3$).

[f] $R_1 = \Sigma||F_o| - |F_c||/\Sigma|F_o|$; $wR_2 = [\Sigma w(F_o^2 - F_c^2)^2/\Sigma w(F_o^4)]^{1/2}$.

Computational Methods

All calculations were carried out using the Gaussian 16 software package.[7] The input structure of (^{Me}IPrCH)Si{Si($SiMe_3$)$_3$} was taken from the molecular structure obtained from X-ray crystallography and first optimized using the B3LYP[8] functional and 6-31G(d,p)[9] basis set in the gas phase. This optimized geometry was subsequently re-optimized using the M06-2X[10] functional and def2-TZVP[11] basis set and confirmed to be a minimum on the potential energy surface using frequency analysis. Natural resonance theory (NRT) analysis was computed using the M06-2X/def2-TZVP optimized structure using the NBO 6.0 program.[12] Only resonance delocalization involving the N_2C=C-Si atoms of the molecule was considered (atoms 2,6,7,9,10) of the atom list given below Figure S31). The reaction coordinate for the formation of (^{Me}IPrCH)Si(P_4){Si($SiMe_3$)$_3$} was calculated at the B3LYP/6-31G(d,p) level using a truncated model where both the -Dipp and -$SiMe_3$ groups were replaced by -CH_3 groups.

Computed mechanism for the activation of P_4 by (^{Me}IMeCH)Si(SiMe$_3$) and comments

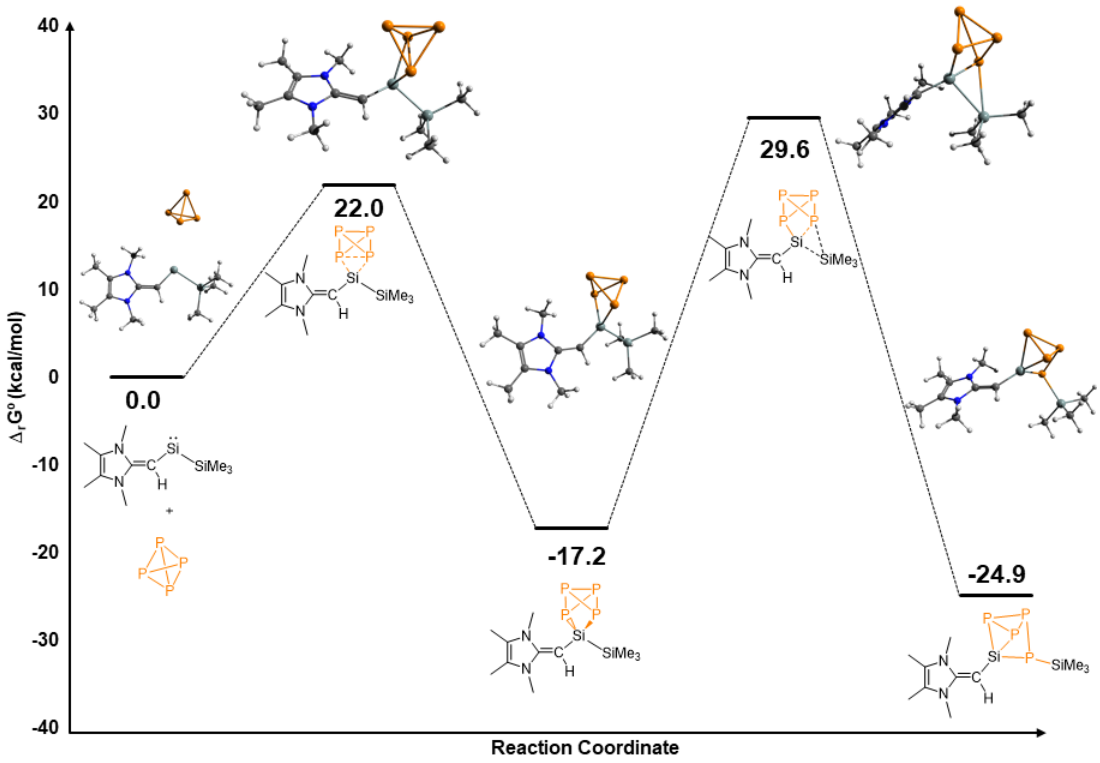

Figure S31. Reaction coordinate diagram for the formation of (^{Me}IMeCH)Si(P_4){SiMe$_3$} from (^{Me}IMeCH)Si(SiMe$_3$) and P_4 at the B3LYP/6-31G(d,p) level of theory.

It should be emphasized that the computed reaction mechanism shown in Figure S32 is meant to illustrate one possible mechanism for the formation of compound ***6****. Notably, the high energy barrier of the second step (46.8 kcal/mol) may be a result of truncation or may suggest that other mechanism(s) are at play. In order elucidate the effect of truncation on this reaction, we attempted to compute the reaction coordinate using the full model. In this case, while reasonable transition states were located, the expected single imaginary vibrational modes of each transition state were located on the bulky -Dipp or -Si(SiMe$_3$)$_3$ substituents rather than along the reaction pathway.*

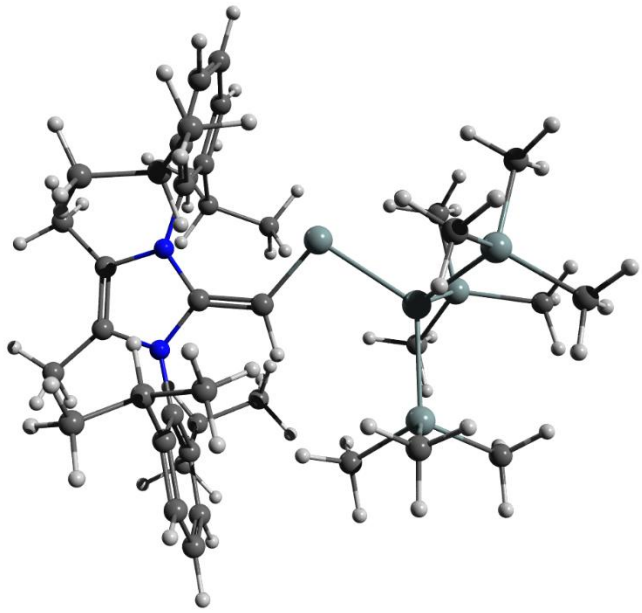

Figure S32. Optimized geometry of (^{Me}IPrCH)Si{Si(SiMe$_3$)$_3$} at the M06-2X/def2-TZVP level of theory.

Si	-2.90699	0.12885	-0.01578
Si	-0.86916	1.32387	-0.38554
Si	-3.15035	-2.19251	-0.21399
Si	-4.53916	1.14766	-1.34146
Si	-3.41336	0.68465	2.20501
N	2.56364	1.07815	-0.10867
N	2.52377	-1.07932	0.00970
C	2.20689	2.46321	-0.13391
C	1.70752	0.01730	-0.05884
C	0.30475	-0.02121	-0.07282
H	-0.04661	-1.03521	0.08673
C	3.89302	0.64508	-0.05030
C	2.04399	-3.21471	1.07327
C	3.86763	-0.70149	0.00594
C	1.76989	-2.94482	-1.35210
C	2.08861	-2.43660	-0.09009
C	1.89249	3.05313	-1.36335
C	1.38885	-4.28246	-1.43067
H	1.12726	-4.70517	-2.39299
C	1.33531	-5.07348	-0.29707
H	1.03436	-6.11020	-0.37678
C	2.21875	3.17038	1.06966

C	2.35739	-2.60683	2.42746
H	3.09687	-1.81666	2.27710
C	4.95696	-1.71077	0.03870
H	4.91372	-2.31812	0.94559
H	5.92530	-1.21673	0.00108
H	4.88130	-2.39231	-0.81112
C	1.66042	-4.54462	0.94312
H	1.61214	-5.17731	1.81902
C	5.02035	1.61160	-0.01182
H	4.95669	2.32858	-0.83203
H	5.96819	1.08221	-0.08315
H	5.01400	2.18403	0.91891
C	1.81331	-2.09383	-2.60595
H	2.19095	-1.10448	-2.33974
C	1.60551	4.41190	-1.36348
H	1.34421	4.90576	-2.28890
C	1.82665	2.22300	-2.63342
H	1.41143	1.25013	-2.35611
C	2.48986	2.48617	2.39602
H	3.02175	1.55234	2.19894
C	1.90701	4.52665	1.01985
H	1.89107	5.10664	1.93333
C	1.61251	5.14108	-0.18403
H	1.37284	6.19650	-0.20445
C	2.94730	-3.60981	3.41556
H	2.20417	-4.34366	3.73185
H	3.28635	-3.08829	4.31124
H	3.79573	-4.14705	2.98819
C	-4.66966	-2.76543	0.74662
H	-4.54053	-2.60669	1.81942
H	-4.84102	-3.83300	0.58379
H	-5.56598	-2.22587	0.43393
C	-1.66576	-3.14077	0.45526
H	-0.80662	-3.06124	-0.21481
H	-1.90700	-4.20261	0.55607
H	-1.36167	-2.76618	1.43537
C	1.10234	-1.94937	3.01033
H	0.69770	-1.19627	2.33196
H	1.32934	-1.46959	3.96442
H	0.32822	-2.70084	3.18261
C	-6.20455	0.26882	-1.24370
H	-6.13523	-0.75601	-1.61455
H	-6.95190	0.79255	-1.84538
H	-6.56719	0.22721	-0.21441
C	3.36352	3.32802	3.32610
H	4.27582	3.66332	2.82983

H	3.64365	2.74280	4.20291
H	2.83104	4.21091	3.68276
C	0.40704	-1.91556	-3.18425
H	-0.01008	-2.87751	-3.49137
H	0.43677	-1.26543	-4.06093
H	-0.26035	-1.46564	-2.44740
C	2.76331	-2.68440	-3.64979
H	3.76922	-2.81066	-3.24660
H	2.82242	-2.02625	-4.51800
H	2.41418	-3.65931	-3.99451
C	1.16665	2.12572	3.07992
H	0.58866	3.03026	3.28248
H	1.35186	1.61808	4.02867
H	0.56421	1.47210	2.44647
C	0.88879	2.82144	-3.67834
H	-0.08382	3.05366	-3.24162
H	0.74060	2.10696	-4.48907
H	1.30279	3.73146	-4.11787
C	-3.96513	1.14407	-3.13668
H	-3.02351	1.69039	-3.23211
H	-4.70122	1.61763	-3.79103
H	-3.79759	0.12557	-3.49346
C	-5.25399	0.54573	2.58568
H	-5.82331	1.27117	2.00031
H	-5.44349	0.74640	3.64353
H	-5.63945	-0.44821	2.35246
C	3.21519	1.98996	-3.23670
H	3.70580	2.94276	-3.44888
H	3.12755	1.43862	-4.17517
H	3.85615	1.41102	-2.57115
C	-4.78006	2.93817	-0.80729
H	-5.21409	2.99707	0.19323
H	-5.44878	3.46167	-1.49525
H	-3.82422	3.46672	-0.79075
C	-3.39790	-2.68893	-2.01629
H	-4.31023	-2.24904	-2.42466
H	-3.48016	-3.77542	-2.10565
H	-2.56203	-2.35996	-2.63645
C	-2.87858	2.45191	2.57897
H	-1.80141	2.57169	2.44232
H	-3.12408	2.71670	3.61096
H	-3.37292	3.16458	1.91619
C	-2.46015	-0.45817	3.36328
H	-2.75198	-1.50235	3.23060
H	-2.63130	-0.18830	4.40854
H	-1.38804	-0.38327	3.16384

References

1. A. B. Pangborn, M. A. Giardello, R. H. Grubbs, R. K. Rosen and F. J. Timmers, *Organometallics*, 1996, **15**, 1518.

2. K. Powers, C. Hering-Junghans, R. McDonald, M. J. Ferguson and E. Rivard, *Polyhedron*, 2016, **108**, 8.

3. C. Marschner, *Eur. J. Inorg. Chem.* 1998, 221.

4. H. Hope, *Prog. Inorg. Chem.*, 1994, **41**, 1.

5. G. M. Sheldrick, *Acta. Crystallogr. Sect. A.*, 2015, **71**, 3.

6. G. M. Sheldrick, *Acta. Crystallogr. Sect. C.*, 2015, **71**, 3

7. Gaussian 16, Revision B.01, M. J. Frisch, G. W. Trucks, H. B. Schlegel, G. E. Scuseria, M. A. Robb, J. R. Cheeseman, G. Scalmani, V. Barone, G. A. Petersson, H. Nakatsuji, X. Li, M. Caricato, A. V. Marenich, J. Bloino, B. G. Janesko, R. Gomperts, B. Mennucci, H. P. Hratchian, J. V. Ortiz, A. F. Izmaylov, J. L. Sonnenberg, D. Williams-Young, F. Ding, F. Lipparini, F. Egidi, J. Goings, B. Peng, A. Petrone, T. Henderson, D. Ranasinghe, V. G. Zakrzewski, J. Gao, N. Rega, G. Zheng, W. Liang, M. Hada, M. Ehara, K. Toyota, R. Fukuda, J. Hasegawa, M. Ishida, T. Nakajima, Y. Honda, O. Kitao, H. Nakai, T. Vreven, K. Throssell, J. A. Montgomery, Jr., J. E. Peralta, F. Ogliaro, M. J. Bearpark, J. J. Heyd, E. N. Brothers, K. N. Kudin, V. N. Staroverov, T. A. Keith, R. Kobayashi, J. Normand, K. Raghavachari, A. P. Rendell, J. C. Burant, S. S. Iyengar, J. Tomasi, M. Cossi, J. M. Millam, M. Klene, C. Adamo, R. Cammi, J. W. Ochterski, R. L. Martin, K. Morokuma, O. Farkas, J. B. Foresman and D. J. Fox, Gaussian, Inc., Wallingford CT, 2016.

8. (*a*) C. Lee, W. Yang and R. G. Parr, *Phys. Rev. B*, 1988, **37**, 785; (*b*) A. D. Becke, *Phys. Rev. A*, 1988, **38**, 3098; (*c*) P. J. Stephens, F. J. Devlin, C. F. Chabalowski and M. J. Frisch, *J. Phys. Chem.*, 1994, **98**, 11623.

9. (*a*) P. C. Hariharan and J. A. Pople, *Theor. Chim. Acta*, 1973, **28**, 213; (b) M. M. Francl, W. J. Pietro, W. J. Hehre, J. S. Binkley, M. S. Gordon, D. J. DeFrees and J. A. Pople, *J. Chem. Phys.*, 1982, **77**, 3654.

10. Y. Zhao and D. G. Truhlar, *Theor. Chem. Acc.*, 2008, **120**, 215

11. F. Weigend and R. Ahlrichs, *Phys. Chem. Chem. Phys.*, 2005, **7**, 3297.

12. NBO 6.0, E. D. Glendening, J, K. Badenhoop, A. E. Reed, J. E. Carpenter, J. A. Bohmann, C. M. Morales, C. R. Landis, F. Weinhold, Theoretical Chemistry Institute, University of Wisconsin, Madison, 2013.